

Alma Mater Studiorum Università di Bologna  
Archivio istituzionale della ricerca

Considerations for evaluating green infrastructure impacts in microscale and macroscale air pollution dispersion models

This is the final peer-reviewed author's accepted manuscript (postprint) of the following publication:

*Published Version:*

Arvin Tiwari, Prashant Kumar, Richard Baldauf, K. Max Zhang, Francesco Pilla, Silvana Di Sabatino, et al. (2019). Considerations for evaluating green infrastructure impacts in microscale and macroscale air pollution dispersion models. *SCIENCE OF THE TOTAL ENVIRONMENT*, 672, 410-426 [10.1016/j.scitotenv.2019.03.350].

*Availability:*

This version is available at: <https://hdl.handle.net/11585/684249> since: 2021-01-29

*Published:*

DOI: <http://doi.org/10.1016/j.scitotenv.2019.03.350>

*Terms of use:*

Some rights reserved. The terms and conditions for the reuse of this version of the manuscript are specified in the publishing policy. For all terms of use and more information see the publisher's website.

This item was downloaded from IRIS Università di Bologna (<https://cris.unibo.it/>).  
When citing, please refer to the published version.

(Article begins on next page)

This is the final peer-reviewed accepted manuscript of:

Arvind Tiwari, Prashant Kumara, Richard Baldauf, Max Zhang, Francesco Pilla, Silvana Di Sabatino, Erika Brattich, Beatrice Pulvirenti, Considerations for evaluating green infrastructure impacts in microscale and macroscale air pollution dispersion models. Science of The Total Environment, Volume 672 (2019), P. 410-426.

The final published version is available online at:

<https://doi.org/10.1016/j.scitotenv.2019.03.350>

© 2019. This manuscript version is made available under the Creative Commons Attribution-NonCommercial-NoDerivs (CC BY-NC-ND) 4.0 International License (<http://creativecommons.org/licenses/by-nc-nd/4.0/>)

*Review article*

## **Considerations for evaluating green infrastructure impacts in microscale and macroscale air pollution dispersion models**

**Arvind Tiwari<sup>a</sup>, Prashant Kumar<sup>a, \*</sup>, Richard Baldauf<sup>b, c</sup>, K Max Zhang<sup>d</sup>, Francesco Pilla<sup>e</sup>, Silvana Di Sabatino<sup>f</sup>, Erika Brattich<sup>f</sup>, Beatrice Pulvirenti<sup>g</sup>**

<sup>a</sup>*Global Centre for Clean Air Research (GCARE), Department of Civil and Environmental Engineering, Faculty of Engineering and Physical Sciences, University of Surrey, Guildford GU2 7XH, United Kingdom*

<sup>b</sup>*U.S. Environmental Protection Agency, Office of Research and Development, Research Triangle Park, NC, USA*

<sup>c</sup>*U.S. Environmental Protection Agency, Office of Transportation and Air Quality, Ann Arbor, MI, USA*

<sup>d</sup>*Sibley School of Mechanical and Aerospace Engineering, Cornell University, Ithaca, New York 14853, United States*

<sup>e</sup>*Department of Planning and Environmental Policy, University College Dublin, Dublin, D14, Ireland*

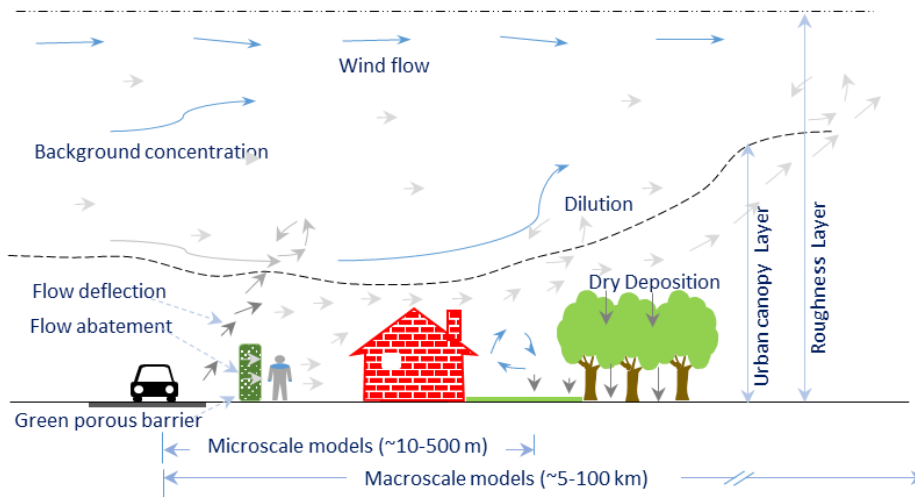
<sup>f</sup>*Department of Physics and Astronomy, Alma Mater Studiorum - University of Bologna, Viale Berti Pichat 6/2, 40127 Bologna, Italy*

<sup>g</sup>*Dipartimento di Ingegneria Energetica, Nucleare e del Controllo Ambientale, University of Bologna, Bologna, Italy*

---

\* Corresponding author. Address as above. E-mail addresses: P.Kumar@surrey.ac.uk, Prashant.Kumar@cantab.net

## Graphical abstract



## Abstract

Green infrastructure (GI) in urban areas may be adopted as a passive control system to reduce air pollutant concentrations. However, current dispersion models offer limited modelling options to evaluate its impact on ambient pollutant concentrations. The scope of this review revolves around the following question: how can GI be considered in readily available dispersion models to allow evaluation of its impacts on pollutant concentrations and health risk assessment? We examined the published literature on the parameterisation of deposition velocities and datasets for both particulate matter and gaseous pollutants that are required for deposition schemes. We evaluated the limitations of different air pollution dispersion models at two spatial scales – microscale (i.e. 10-500m) and macroscale (i.e. 5-100km) - in considering the effects of GI on air pollutant concentrations and exposure alteration. We conclude that the deposition schemes that represent GI impacts in detail are complex, resource-intensive, and involve an abundant volume of input data. An appropriate handling of GI characteristics (such as aerodynamic effect, deposition of air pollutants and surface roughness) in dispersion models is necessary for understanding the mechanism of air pollutant concentrations simulation in

presence of GI at different spatial scales. The impacts of GI on air pollutant concentrations and health risk assessment (e.g., mortality, morbidity) are partly explored. The i-Tree tool with the BenMap model has been used to estimate the health outcomes of annually-averaged air pollutant removed by deposition over GI canopies at the macroscale. However, studies relating air pollution health risk assessments due to GI-related changes in short-term exposure, via pollutant concentrations redistribution at the microscale and enhanced atmospheric pollutant dilution by increased surface roughness at the macroscale, along with deposition, are rare. Suitable treatments of all physical and chemical processes in coupled dispersion-deposition models and assessments against real-world scenarios are vital for health risk assessments.

**Keywords:** Microscale model; Macroscale model; Green infrastructure; Deposition velocity; dispersion-deposition coupled model; Air pollution health risk assessment

## 1. Introduction

Green infrastructure (GI) is broadly intended a combination of green, manufactured or natural elements such as green roofs, green facades, grasslands, hedges, individual trees or plants at species-level that can be implemented in real urban environments to improve aesthetic appearance of the environment where we live in, improve the possibility of amenities but also to potentially improve environmental health conditions. The term GI may have different meanings in different contexts. For instance, eco-friendly construction that has a low-carbon footprint and increased energy efficiency are also often defined as green buildings/infrastructure in structural engineering. At the same time, in Geo-environment engineering, GI is a group of trees and plants used to limit soil erosion. Benedict and McMahon (2002) defined GI “as an interconnected network of green space that conserves natural ecosystem values and functions and provides associated benefits to human populations”. For urban air quality, the most important forms of GI are street trees, roadside hedges, green walls and roofs, parks and grasslands adjacent to the urban boundary where air exchange is

significant. In this review, we focus only on forms of urban GI that includes groups of trees, plants and/or hedges with a large leaf area index (LAI;  $\text{m}^2 \text{m}^{-2}$ ), with an aim to draw critical discussion points on how these GI forms could be considered in various readily-available dispersion models used for air quality and health impact assessments.

Traffic emissions are a major source of air pollution in urban areas and adversely impact upon human health and the environment (Kumar et al., 2016, 2015, 2013). Adverse health effects have been linked to exposures of regulated air pollutants such as particulate matter including  $\text{PM}_{10}$  (fraction of particles with an aerodynamic diameter  $\leq 10\mu\text{m}$ ; Talbi et al., 2018),  $\text{PM}_{2.5}$  (fraction of particles with an aerodynamic diameter  $\leq 2.5\mu\text{m}$ ; Rivas et al., 2017), Ozone ( $\text{O}_3$ ; Goodman et al., 2018), nitrogen dioxides ( $\text{NO}_x$ ; Jeanjean et al., 2017; Muttoo et al., 2018) and unregulated pollutants such as ultrafine particles (UFP; Baldauf et al., 2016; Kumar et al., 2017; Pacitto et al., 2018), black carbon (Rivas et al., 2017), volatile organic compounds (VOCs; McDonald et al., 2018) and heavy metals (Aksu, 2015; Onder and Dursun, 2006).

Recent studies have shown potential of GI for improving near-road air quality and limiting personal exposures to local air pollution sources (Abhijith and Kumar, 2019; Abhijith et al., 2017; Baldauf, 2017). GI can reduce pollutant concentrations by offering a greater surface area for increased dry deposition, enhancing pollutant redistribution and increasing atmospheric turbulence, although some GI characteristics can strengthen atmospheric stagnation and increase local air pollution concentrations (Deshmukh et al., 2018; Steffens et al., 2012). Without the GI, dispersion of air pollution is governed by factors, such as wind speed and direction, topography and meteorology. GI can add additional dispersion characteristics by their surface roughness, geometry and deposition characteristics. A potential reduction of air pollutant concentrations led by these processes has been reported at both microscale (i.e. 10-500 m; Britter and Hanna, 2003) in street canyon environment (Gromke et al., 2016; Pugh et

al., 2012) and at the citywide macroscale (i.e. 5-100 km; Bottalico et al., 2017; Currie and Bass, 2008; Nowak, 1994). For example, Pugh et al. (2012) used CFD simulation for studying the effect of green wall and roof on air pollutant reduction in street canyons. They found that the presence of green wall and roof together could reduce NO<sub>2</sub> and PM concentrations as much as 40% and 60%, respectively, depending upon the street canyon aspect ratio. Later, Gromke et al. (2016) simulated the effect of hedgerows in a wind tunnel for assessing the personal exposure reduction in street canyons with an aspect ratio (i.e., width to building height) of two. They showed that discontinuous hedgerows could result in increased air pollutant concentrations in the range of 3-19% compared to no hedgerow scenario. Abhijith et al. (2017) summarised positives and downsides in terms of air quality in different environments and highlights a need for careful selection of GI under diverse urban conditions. At macroscale, Bottalico et al. (2017) studied the importance of urban forest in air purification in Florence, Italy. They used remote sensing data and applied a regression model to map urban forest and LAI, in addition, to estimating the deposited amount of O<sub>3</sub> and PM<sub>10</sub>. Their results show that the urban forest can remove air pollutant concentrations monthly up to 5% of O<sub>3</sub> and 13% of PM<sub>10</sub>. Summary of relevant studies considering GI modelling at the microscale and macroscale is presented in Table 1. It is worth noting the large reductions at the microscale are usually for shorter averaging times while the macroscale assessments are generally for annual averages. Also, these are for different vegetation characteristics and therefore there are no direct comparisons between the reductions at these two scales. The assessments that have carried out comparisons of short- and long-term benefits from similar vegetation characteristics are currently lacking in the literature.

The underlining reasons for air pollutant concentration reductions are led by complex processes, such as enhanced dilution due to enhanced atmospheric turbulence owing to increased surface roughness (Pleijel et al., 2004), air pollutants concentration redistribution (Abhijith et al., 2017;

Baldauf, 2017) and dry deposition which is strongly influenced by LAI (Jayasooriya et al., 2017; Selmi et al., 2016). To identify the dominant process of GI's effects on air pollution would require a specially-designed experiment measuring air pollutant reductions at different distances from the source in combination with different GI types and characteristics (Deshmukh et al., 2018). Coupled GI and air pollutant dispersion modelling to estimate associated dry deposition is based on consideration of GI as a porous medium in CFD (Jeanjean et al., 2015) and wind tunnel (Gromke et al., 2012) simulations, as a whole in receptor models (Chen et al., 2016; Li et al., 2016; Maleki et al., 2016), time of interaction (Pugh et al., 2012) and air pollutant concentration over the surface area (Jeanjean et al., 2016; Tiwary et al., 2009). At macroscale, the dilution of air pollutants due to GI-induced enhanced atmospheric turbulence has not been studied much, but some previous works already established a potential decrease in ground level air pollutant concentration with increasing surface roughness (Barnes et al., 2014; Venkatram et al., 2013). Past works have also investigated the impacts of GI on the reduction of particulate matter (Janhäll, 2015), urban heat island mitigation (Akbari et al., 2001; Bowler et al., 2010; Luber and McGeehin, 2008), reductions in noise pollution (Chiesura, 2004; Pathak et al., 2011), reductions in pollutant exposure as passive roadside barriers (Abhijith et al., 2017; Gallagher et al., 2015, 2013), stormwater management (Czemiel Berndtsson, 2010; Shaneyfelt et al., 2017), and the consideration of GI as a part of natural capital (Chenoweth et al., 2018).

However, uncertainty in GI modelling may lead to overestimation of total dry deposition, which can result in an under-prediction of exposure. For instance, the use of constant surface resistance in a dispersion modelling would overestimate dry deposition by approximately ten-fold (Cape et al., 2008), while low-resolution concentration data in deposition models can lead to overestimation by a factor of two (Schrader et al., 2018). Therefore, it is essential to consolidate and synthesise previous investigations on the considerations of GI in micro and

macro scale air pollutant dispersion model for: (i) researchers to identify knowledge gaps for improved coupled modelling of air pollutant deposition and dispersion in atmospheric models, and (ii) decision-makers to assess the potential of GI to evaluate air quality and health benefits and incorporate findings accordingly into future urban planning. We summarise potential considerations in the microscale and macroscale air pollution modelling regarding GI. These summaries can assist in the formulation of coupled models to obtain a more realistic estimate of atmospheric chemical budgets.

Furthermore, previous articles on interactions between GI and air pollutants have discussed: current methods of estimating dry deposition with numerical models (Wesely, 2000); applications of atmospheric models for particle dispersion (Holmes and Morawska, 2006); assessment of deposition velocities of air pollutants to different vegetation species (Hirabayashi et al., 2011); methods and controlling factors for particulate matter dry deposition (Mohan, 2016); assessment of deposition and thermal effects of urban trees (Buccolieri et al., 2018); bi-directional air pollutant exchange between GI and the atmosphere (Massad et al., 2010); detrimental effects of particulate matters on GI (Litschke and Kuttler, 2008); and estimation of deposition velocities based on land use (Schrader and Brümmer, 2014). However, there remains a need to estimate GI-related dry deposition in atmospheric dispersion models for both the microscale and macroscale. Janhäll (2015) provided a thorough literature review on urban GI effects on particulate matter concentrations at different spatial scales. Our review extends its scope by focusing on the importance of different resistances in the estimation of deposition velocity for both gaseous pollutants and particulate matter and their consideration in coupled dispersion-deposition modelling. In particular, we: (i) carry out a detailed review of parameterisation for GI modelling to estimate deposition velocity; (ii) provide a comprehensive summary of design inputs (e.g., meteorological, GI, and topographical parameters) to evaluate the different respective resistance and deposition velocity for their estimation by deposition

models; (iii) evaluate the effectiveness of microscale and macroscale air pollution dispersion models to estimate pollutant concentration reductions by GI; (iv) evaluate the parametric uncertainties in coupled GI and dispersion modelling; and (v) discuss a numerical framework for linking GI, air pollution and public health outcomes.

## **2. Scope and outline**

This review focuses on GI that includes vegetation (trees, hedges and bushes in street canyons or at open roadsides), grasslands including parks and gardens and urban forests both within microscale and macroscale. The direction of deposition velocity for green walls and inclined roofs is not usually perpendicular to the implanted surfaces. Therefore, a discussion on green walls, inclined roofs or any other artificial system, as well as considerations of wind direction impacts are kept out of the scope of this study.

We carried out a systematic literature review by searching articles using Google Scholar, Scopus, Web of Science, and Science Direct in addition to those known to authors. The following keywords were used in our search: dry deposition, green infrastructure, air pollution and trees, air pollutant dispersion models, air transport models, air pollution and vegetation, deposition velocity, air pollution exposure assessment, urban tree and health benefits, roadside vegetation, air pollution and health, microscale and macroscale simulation. We considered a period over the past three decades (1973-2019) and those written in English language. The outputs of the search were manually screened and those fitting directly to the topic areas and context of the article were selected for discussion.

The review starts by critically synthesising GI modelling systems and relevant technical input parameters that are required for the deposition scheme (Section 3). Considerations of GI in air pollution dispersion models at microscale and macroscale to predict spatio-temporal concentrations are discussed at length in Sections 4 and 5, respectively. Section 6 describes

challenges in the simulation of real-world scenarios such as GI deposition velocity, GI spatial distributions, the influence of local meteorological parameters and pollutant transformation. Section 7 focuses on mathematical approaches linking GI, air pollution and public health outcomes. Finally, a summary of topic areas covered, conclusions reached and an outlook for future research is provided in Section 8.

### **3. Deposition scheme in GI modelling systems**

The deposition schemes, which are a part of air transport models, use mathematical equations to describe atmospheric turbulence, absorption (for gases) and gravitational settling (for particles) processes within the atmospheric mixing layer, that estimate the accumulated quantity of air pollutant removal over any solid surface area without involving water in the atmosphere. The following specific conditions make GI considerations distinct in typical numerical simulations: (i) aerodynamic effects in the form of air pollutant concentration redistributions (Hefny et al., 2015); (ii) deposition of air pollutants (Nowak et al., 2018); and (iii) surface roughness affecting atmospheric turbulence (Barnes et al., 2014). At the microscale, roadside GI such as hedges may act as a filtering barrier between air pollution sources and receptors that can reduce personal exposures for nearby populations. However, at the macroscale, GI such as urban forests, parks, gardens and hedges collectively increase atmospheric dilution as well as act as a sink (in terms of deposition) for atmospheric pollutants. Harmful gaseous pollutants and airborne particles deposit while passing over the GI surface. Since there is no globally accepted deposition scheme to describe the dry deposition process due to the complexity of air pollutants-GI interaction that influence the deposition flux, we discussed dry deposition schemes to identify sets of data required for covering various scenarios. The pollutant flux ( $F$ ;  $\text{g m}^{-2} \text{s}^{-1}$ ) to GI is proportional to the deposition velocity ( $V_d$ ;  $\text{m s}^{-1}$ ) and pollutant concentration ( $C$ ;  $\text{g m}^{-3}$ ) (Bottalico et al., 2016; Jeanjean et al., 2016; Tiwary et al., 2009).

$$F = V_d \times C \quad (1)$$

$V_d$  for different gaseous pollutant (Eq. 2) can be calculated as the inverse sum of aerodynamic resistance ( $R_a$ ;  $s\ m^{-1}$ ), quasi-laminar boundary layer resistance ( $R_b$ ;  $s\ m^{-1}$ ) and the vegetation canopy resistance ( $R_c$ ;  $s\ m^{-1}$ ) (Janhäll, 2015; Tallis et al., 2011; Tiwary et al., 2009).

$$V_d = \frac{1}{R_a + R_b + R_c} \text{ for gaseous pollutants} \quad (2)$$

For particulate matter (Eq. 3), Giardina *et al.* (2018) have proposed a new deposition model based on an electrical analogy scheme to estimate  $V_d$  by using both total resistance  $R_z (= R_a + R_{bp}$ ;  $s\ m^{-1}$ ) and settling velocity ( $V_s$ ;  $m\ s^{-1}$ ) (Eq. 3). The schematic diagram for gaseous pollutant collection, through dry deposition, as represented in Fig 1.

$$V_d = \frac{V_s}{1 - e^{-(R_z V_s)}} \text{ for particulate matter} \quad (3)$$

The  $R_a$  depends on the atmospheric turbulence over the surface and is independent on the species (Eq. 4). The influences of  $R_a$  typically dominate from 10 to 100 m above the ground level (Cherin et al., 2015; Padro and Edwards, 1991; Zhang et al., 2017a).

$$R_a = \frac{1}{k u_*} \left( \ln \frac{z_h}{z_0} - \Psi_h \right) \quad (4)$$

Where  $k$  (-) is the von Karman constant (0.4);  $Z_h$  (m) is the reference height;  $z_0$  (m) is the aerodynamic surface roughness height above the displacement plane;  $u_*$  ( $m\ s^{-1}$ ) is the friction velocity depending upon the atmospheric turbulence and  $\Psi_h$  (-) is a stability function of momentum depend on the Pasquill stability class calculated based on Monin-Obukhov length ( $L$ ; m) using Eq. (5):

$$L = \frac{u_*^3 c_p \rho \bar{T}}{kgH} \quad (5)$$

$c_p$  ( $J\ K^{-1}\ kg^{-1}$ ) is the specific heat at constant pressure;  $\bar{T}$  (K) is the average temperature; and  $H$  ( $W\ m^{-2}$ ) is the sensible heat (Koloskov et al., 2007).

$R_b$  and  $R_{bp}$  ( $s\ m^{-1}$ ) affects the deposition of air adjacent to the surface and depend on molecular properties of the pollutant and roughness of the surface (Eqs. 6 and 7 for gaseous pollutant and particulate matter, respectively), with influences typically dominating from 0 to 10 cm above the deposition surface (Giardina and Buffa, 2018; Zhang et al., 2017a).

$$R_b = \frac{2\ Sc^{\frac{2}{3}}}{Pr^{\frac{2}{3}}\ ku_*} \quad \text{for gaseous pollutants} \quad (6)$$

$Sc$  (-) is the Schmidt number ( $\nu/D$ ), where  $\nu$  ( $m^2\ s^{-1}$ ) is the kinematic viscosity of air and  $D$  ( $m^2\ s^{-1}$ ) is the molecular diffusivity of the pollutant, determined from Stokes-Einstein equation ( $D = \frac{kTC_c}{3\pi\mu D_p}$ ), with  $K$  ( $J\ K^{-1}$ ) the Boltzmann constant,  $T$  ( $K$ ) the absolute temperature,  $\mu$  ( $kg\ m^{-1}\ s^{-1}$ ) the air dynamic viscosity, and  $C_c$  (-) the Cunningham factor and  $Pr$  the Prandtl number ( $= \frac{C_p \nu}{k}$ ) with  $C_p$  the heat capacity per unit volume of the air,  $\nu$  the kinematic viscosity, and  $k$  ( $W\ m^{-1}\ K^{-1}$ ) the thermal conductivity.

$$\frac{1}{R_{bp}} = \left( \frac{1}{R_{bd}} + \frac{1}{R_{bi}} + \frac{1}{R_{bi}+R_{bt}} \right) \quad \text{for particulate matter} \quad (7)$$

$R_{bd}$  ( $s\ m^{-1}$ ) is dependent on the Schmidt number,  $R_{bi}$  ( $s\ m^{-1}$ ) on the surface conditions and Stokes number, and  $R_{bt}$  ( $s\ m^{-1}$ ) on the dimensionless particle relaxation time.

The  $R_c$  is the most uncertain resistance and varies with the nature of the surface and the type of GI (Fowler, 1981; Hirabayashi et al., 2012; Janhäll, 2015; Jayasooriya et al., 2017; Nowak et al., 2006; Wesely, 1989; Zhang et al., 2003). Most of the deposition models found in the literature used Eq. (8) to evaluate canopy resistance for the gaseous pollutant (Seinfeld and Pandis, 2006; Walmsley and Wesely, 1996; Wesely, 1989; Zhang et al., 2017a).

$$\frac{1}{R_c} = \frac{1}{R_s+R_m} + \frac{1}{R_{lu}} + \frac{1}{R_{dc}+R_{cl}} + \frac{1}{R_{ac}+R_{gs}} \quad (8)$$

When gaseous pollutants enter the substomatal cavity in leaves, the diffusion of gaseous material is resisted through the stomata of the leaves, known as stomatal resistance ( $R_s$ ;  $s\ m^{-1}$ ) and through aqueous media of the spongy mesophyll cells, known as mesophyll resistance ( $R_m$ ;

$\text{s m}^{-1}$ ). Zhang *et al.* (2017a) reported the empirical Eq. (9) based on Wesely (1989) to assess the stomatal resistance for GI.

$$R_s = R_i \left( 1 + \frac{1}{200((G+0.1)^2)} \right) \frac{400}{T_s(40-T_s)} \frac{D_{H_2O}}{D_x} \quad (9)$$

$R_i$  ( $\text{s m}^{-1}$ ) is the minimum canopy stomatal resistance depending on land cover,  $G$  ( $\text{W m}^{-2}$ ) is the solar radiation,  $T_s$  ( $^{\circ}\text{C}$ ) is the surface temperature, and  $D_{H_2O}/D_x$  (-) is the ratio of diffusivity between the water vapour and the gaseous pollutant.  $R_s$  is primarily a function of the size of the stomata and time of opening or closing of the stomata based on the plants' photosynthesis requirement (Zhang et al., 2017a).  $R_m$  is dependent on the chemical properties of the pollutant, such as solubility, reactivity and the type of vegetation species. While interacting within mesophyll cells, pollutants transform from air to liquid and then diffuse into the aqueous media of the spongy mesophyll cells. Xiao and Zhu (2017) recognised that the pollutant, after entering the substomatal cavity, experiences resistance from the physical barriers and biochemical components inside the cell wall, chloroplast envelope, cytosol and stroma between substomatal cavity, and the chloroplast of the leaf, which can be modelled with Eq. (10).

$$R_m = \frac{RT}{H_c} R_{air} + R_{liq} \quad (10)$$

Where  $R$  ( $\text{bar m}^3 \text{K}^{-1} \text{mol}^{-1}$ ) the gas constant;  $T$  the absolute temperature of air;  $H_c$  ( $\text{bar m}^3 \text{mol}^{-1}$ ) the Henry law constant (which is a dimensionless number used to convert  $R_{air}$  to its liquid-phase equivalent resistance); and  $R_{liq}$  ( $\text{s m}^{-1}$ ) the summation of all series of liquid resistances (resistance of the cell wall and membrane, resistance of the cytosol between the chloroplast and the cell wall, resistance of the chloroplast envelope and resistance of the stroma).

Other than stomatal openings, the available deposition surface of most leaves comprises a waxy top layer of the cuticle known as the cutin polyester membrane (Ruggiero et al., 2017), while the related resistance to deposition is known as a cuticle or cuticular resistance ( $R_{lu}$ ;  $\text{s m}^{-1}$ ). Since the permeation of air pollutants through cuticles are negligible (Grünhage and Haenel,

1997), the resistance is an order less than stomatal resistances (Wesely and Hicks, 1977). The value of cuticle resistance is subjected to a degree of wetness of the surface and pH value (Massad et al., 2010) which can be divided into dry cuticle resistance and wet cuticle resistance (Walmsley and Wesely, 1996). A single model to evaluate the cuticle resistance for a wide range of GI, organs or pollution conditions are not possible because deposition and gas exchange phenomena are functions of wettability, the degree of polarity and apolarity of the plant surfaces, retention and quality of surface-deposited liquids (Fernández et al., 2017). Zhang *et al* (2002) have estimated cuticle resistance for dry and wet conditions by Eqs. (11) and (12), respectively.

$$R_{lu\ dry} = \frac{R_{lu\ dry0}}{e^{0.03RH} LAI^{1/4} u_*} \quad (11)$$

$$R_{lu\ wet} = \frac{R_{lu\ wet0}}{LAI^{1/2} u_*} \quad (12)$$

Where  $R_{lu\ dry0}$  ( $s\ m^{-1}$ ) and  $R_{lu\ wet0}$  ( $s\ m^{-1}$ ) are reference values of dry and wet cuticle resistance, that vary with GI type.

Due to the porosity of GI, air pollutants may enter into the lower canopy of dense vegetation, where atmospheric buoyancy resistance ( $R_{dc}$ ;  $s\ m^{-1}$ ) is dominated by buoyant convection forces, which depend on the amount of sunlight that heats the surface or lower canopy, and the angle of the terrain (Eq. 13).

$$R_{dc} = 100 \left( 1 + \frac{1000}{G+10} \right) \times (1 + 1000\theta)^{-1} \quad (13)$$

Where  $\theta$  is the slope of the local terrain in radians. Although  $R_{dc}$  in the lower canopy is independent of wind speed, in cases when winds are able to penetrate into the lower canopy, especially on the sides of hills, could change the mixing force (Wesely, 1989).

Resistance to the uptake of air pollutants by leaves, twigs, bark and other exposed surfaces within the lower canopy is known as lower canopy resistance ( $R_{cl}$ ;  $s\ m^{-1}$ ).  $R_{cl}$  depends on

canopy structure metric such as bark area index, porosity and areal density. Zhang *et al.* (2017a) reported Eq. (14) to estimate the  $R_{cl}$  as:

$$R_{cl} = \left( \frac{10^{-5}H_c}{R_{cl,SO_2}} + \frac{f_0}{R_{cl,O_3}} \right)^{-1} \quad (14)$$

$f_0$  (-) is the reactivity factor for gases,  $R_{cl,SO_2}$  ( $s\ m^{-1}$ ) and  $R_{cl,O_3}$  ( $s\ m^{-1}$ ) denote the baseline  $R_{cl}$  for  $SO_2$  and  $O_3$ , respectively, as given in Wesely (1988).

Many deposition models assume that deposition to the ground surface under GI is negligible but some research findings indicate that the amount of deposition at the surface varies from 20-30% depending on the type of air pollutants (Meyers and Baldocchi, 1988). The resistance offered by GI to an air pollutant while passing through the canopy to the ground surface is known as in-canopy resistance ( $R_{ac}$ ;  $s\ m^{-1}$ ).  $R_{ac}$  is a function of canopy height and LAI of GI and can be modelled using Eq. (15) (Erisman *et al.*, 1994).

$$R_{ac} = \frac{h_c b_c LAI}{u_*} \quad (15)$$

Canopy height,  $h_c$  (m), is the height above ground-level to the top of the GI and  $b_c$  (-) is an empirical constant taken as  $14\ m^{-1}$ .

Canopy soil resistance ( $R_{gs}$ ;  $s\ m^{-1}$ ) is a resistance to the uptake of air pollutants by the soil surface. The deposition of air pollutants depends on the pH value of the soil, relative humidity, surface temperature, soil moisture content, ambient air pollutant concentration, pollutant type and solar radiation (Erisman *et al.*, 1994). The soil resistance,  $R_{soil}$  is similar to the canopy soil resistance and its parameterisation is given by Eq. (16) (Jacobson, 2005).

$$R_{gs}/R_{soil} = \left( \frac{10^{-5}H_c}{R_{gs,SO_2}} + \frac{f_0}{R_{gs,O_3}} \right)^{-1} \quad (16)$$

$R_{gs,SO_2}$  ( $s\ m^{-1}$ ) and  $R_{gs,O_3}$  ( $s\ m^{-1}$ ) denote the baseline soil resistances for  $SO_2$  and  $O_3$ , respectively, as provided in Wesely (1988). Surface resistance ( $R_s$ ;  $s\ m^{-1}$ ) accounts for the amount of air pollutant deposition to any surface including soil, snow and concrete. Canopy

resistance is also a subpart of the  $R_s$ . Erisman (1994) reported temperature-dependent, (Eqs. 17-18) snow-covered  $R_s$  for  $\text{SO}_2$  and  $\text{NH}_3$  as:

$$R_{\text{snow}} = 500 \text{ sm}^{-1} \text{ at } T < -1 \text{ }^\circ\text{C} \quad (17)$$

$$R_{\text{snow}} = 70 (2 - T) \text{ sm}^{-1} \text{ at } -1 < T < 1 \text{ }^\circ\text{C} \quad (18)$$

For particles, the additional parameter  $V_s$ , is required to estimate  $V_d$ , for particle diameters up to 50  $\mu\text{m}$  according to the Stokes law (Eq. 19)

$$V_s = \frac{d_p^2 g (\rho_p - \rho_a) C_c}{18 \mu_a} \quad (19)$$

Where  $\rho_p$  ( $\text{kg m}^{-3}$ ) is the density of the particles,  $\rho_a$  ( $\text{kg m}^{-3}$ ) is the density of the ambient air,  $d_p$  ( $\text{m}$ ) is particle diameter, and  $g$  ( $\text{m s}^{-2}$ ) is the gravitational acceleration.

Alternative methods to evaluate the resistances used for dry deposition estimation for gaseous pollutants are also reported in the literature (Alfieri et al., 2008; Bennett et al., 1973; Ganzeveld and Lelieveld, 1995; Gong et al., 2017; Irmak and Mutiibwa, 2010; Jiang et al., 2017; Kerstiens, 2006; Kumar et al., 2014; Lhomme and Montes, 2014; Magnani et al., 1998; O'Dell et al., 1977; Rodný et al., 2016; Wesely, 1989; Wong et al., 2018; Zhang and Shao, 2014; Zhou et al., 2017). Khan *et al.* (2017) have discussed other models for dry particle deposition schemes. A summary of typical values for different resistances are listed in Supplementary Information (SI) Table S1, while parameters required for dry deposition estimation are summarised in Table 2.

The most widely used deposition model is i-Tree Eco ([www.itreetools.org](http://www.itreetools.org)) that maps the measured air pollutant concentrations by monitoring stations over GI canopies then estimates air pollutant sequestration rates based on air pollutant concentrations, LAI of the GI and meteorological data. For example, Selmi et al. (2016) estimated 88 t of air pollutants removal by urban trees during one year (July 2012 to June 2013) in Strasbourg city, France. However, the i-Tree Eco model does not consider the influence of GI on pollutant dispersion aspects such

as air pollutants redistribution and enhanced atmospheric dilution.

#### **4. Considerations of GI in microscale models**

Microscale models are used to predict air quality near the source, where air pollutant dispersion is dominated by characteristics including source-induced turbulence, pollutant chemistry, local meteorology, source geometry and the surrounding buildings, terrain and GI, flow alternation and many more aspects. In street canyons, aerodynamic effects have a greater impact on local air pollution levels than deposition (Vos et al., 2013). However, in open road conditions, both aerodynamic and deposition effects are important (Tong et al., 2016). In this section, we review several models developed to estimate exposure concentrations, near to traffic emissions, for local populations by capturing the temporal and spatial variation of air pollutant concentrations at the microscale, and we discuss how these models represent GI in their simulation. Although these models were not developed to study the impact of GI on exposures reduction, their results could still be partially used to assess the GI impacts of air pollutant concentrations. Table 3 presents a summary of the differences in GI considerations by various microscale models that are described in the subsequent text.

*Box and wind tunnel models* are based on the principle of conservation. Physical and chemical processes of air pollutant dispersion, dilution and deposition are simulated in the study domain, which is assumed to be isolated from its surroundings. The consideration of roadside GI in microscale models (especially regarding urban street canyons) was intensively studied through laboratory experiments in a wind tunnel by Gromke and co-workers (Gromke, 2011; Gromke et al., 2012; Gromke and Blocken, 2015; Gromke and Ruck, 2007). In these models, air pollutants were forced to pass normally through the vegetation, which was shown to increase the deposition velocity by allowing more time and amount of pollutant to interact with the GI (Janhäll, 2015). However, under ambient conditions, air pollutants only interact with the

available surface area of GI while passing above or around the structure (Abhijith et al., 2017). Moreover, synthetic materials were used to represent GI, which introduced uncertainties in the simulation of  $R_c$ .

*Gaussian plume models* are most commonly used as dispersion models to estimate concentrations of air pollutants by solving a set of mathematical equations in three dimensions, usually considering a point sources. Historically, to incorporate stability conditions and plume rise, the models can use one of five stability classification schemes (Lapse Rate scheme, Pasquill-Gifford scheme, Turner scheme, Sigma-Theta scheme and Richardson number) and one of two (Briggs and Holland method) plume rise formulations (Awasthi et al., 2006). These models also have two different vertical and horizontal dispersion coefficients to simulate vertical and horizontal dilution, depending on stability class and distance from the source. In Gaussian models, the air pollutant concentrations were calculated independently of GI characteristics. With computational advancement, Gaussian plume model limitations have been minimised in modified/advanced models that estimate pollutant concentrations with a combination of different sources' contributions, which are spatially distributed sources (such as multiple points, line and area sources). These models use meteorological data and surface roughness height to compute surface friction velocity, Monin- Obukhov length and the wind speed and direction at a reference height to define atmospheric boundary layer properties and use modified vertical and horizontal dispersion coefficient based on wind tunnel, field experiments or empirically. One dispersion model, RLINE (developed by United States Environmental Protection Agency (US-EPA)), takes meteorological input from AERMET (Cimorelli et al., 2005), vertical and horizontal dispersion with empirical constants obtain based on field tracer studies and wind tunnel simulation (Venkatram et al., 2013) and have been tested against independent field studies (Snyder et al., 2013). RLINE model does not incorporate the effect of GI (roadside vegetation), but it can quantify the effect of roadside barriers on the

prediction of air pollutant concentrations due to modified dispersion coefficients. HIWAY-2 (developed by US-EPA) uses the steady-state Gaussian model to estimate the concentration of nonreactive pollutants from highway traffic at receptors located in relatively uncomplicated terrain; thus, the model is unable to consider complex terrain that includes GI (Peterson, 1980). This model uses only three stability classes (unstable, neutral and stable) and more realistic concentration estimation adjacent to highways with respect to the original version due to updated dispersion coefficients (Peterson, 1980; Sharma and Khare, 2001). Other Gaussian models also use modified dispersion coefficients to include the effect of non-porous barriers. ADMS-Road (developed by the Cambridge Environmental Research Consultants, UK) is a Gaussian plume air dispersion model that uses the boundary layer depth and Monin-Obukhov length to define the atmospheric boundary layer properties, rather than the simplistic Pasquill-Gifford stability classes. This model calculates dry deposition removal by estimating  $R_a$  and  $R_b$  components and uses a constant value of  $R_c$  for the whole modelled domain, which could lead to uncertainty in air pollutant concentrations predictions (Apsley, 2017). Usually, advanced Gaussian models are not capable to simulate the aerodynamic effects of GI, which dominate the spatial distribution of air pollutant at the microscale.

*Receptor models* are applications of a set of mathematical or statistical relationships obtain information on the sources of air pollutants from air pollutants measured at the receptor point. The name receptor models or receptor-oriented models arises from the fact that these methods are focused on the behaviour of the ambient environment at the point of impact as opposed to the source-oriented dispersion models that focus on the emissions, transport, dilution and transformations that occur beginning at the source and following the pollutants to the sampling or receptor sites. Watson *et al.* (2002) have described the procedures for using a receptor model to estimate the contribution of sources at receptor locations. Receptor models are simple, self-explanatory and highly precise in estimating air pollutant concentrations at the receptor point (Watson, 1984).

Many studies (Belis et al., 2013; Gardner and Dorling, 1999; Han et al., 2004; Liu et al., 1996; Song et al., 2001; Wåhlin et al., 2006; Wahlin et al., 2001) reported the application of receptor modelling for air pollutant concentrations simulation. Receptor models can be used to quantify the potential influences of GI as a whole (Chen et al., 2016, 2015; Heal et al., 2012; Li et al., 2016; Maleki et al., 2016; Yin et al., 2011), but in simulating air pollutant concentrations, they are unable to handle the non-linear behaviours of dry deposition, spatial distribution of GI and other parameters such as complex local meteorological parameters, air moisture and wind velocity.

*Computational Fluid Dynamics* (CFD) models are effective and powerful tools for the numerical simulation of wind flow and mass transfer numerically. Most CFD models solve the governing nonlinear Navier Stokes equations, which are conservation of mass, momentum and energy, along with transport and/or any other user specific equations, with the help of any conventional methods such as the Finite Volume Method, Finite Element Method, Finite Difference Method and Spectral Methods. Many CFD models (Amorim et al., 2013; Baik et al., 2009; Costabile et al., 2006; Jeanjean et al., 2017, 2015; Kwak et al., 2018; Marciotto et al., 2010; Sanchez et al., 2016) have also been developed by researchers to simulate complex wind flows and pollutant transfer problems at different scales. Although CFD modelling has the capacity to deal with complex geometries, wind-induced turbulence and air pollutant transformations in simulating air pollutant concentrations (Amorim et al., 2013; Costabile et al., 2006; Jeanjean et al., 2015; Kwak et al., 2018; Lateb et al., 2016; Sanchez et al., 2016), they still require more validation to simulate the effects of modelled geometries on wind velocity and air pollutant concentration predictions in urban settings (Huang et al., 2009; Sini et al., 1996). GI is considered to be a porous media, and its pollutant removal efficiency is modelled as a function of LAI or of Leaf Area Density (LAD;  $\text{m}^2 \text{m}^{-3}$ ) by assuming a constant deposition velocity (Jeanjean et al., 2017; Pugh et al., 2012). However, the aerodynamic effects

(such as momentum sink, local turbulence and transpiration cooling) are also modelled as a function of GI characteristics, as discussed in SI Section S2. Steffens et al. (2012) reported the modeling study on the effect of vegetation barriers on plume dispersion near roadways through coupling turbulence and aerosol dynamics to capture both the aerodynamic and deposition effects. The modeling results show that GI barriers can reduce UFP concentrations, but the level of reduction depends on meteorological conditions. For example, increased wind speed leads to more reduction in particles larger than ~50 nm, but minimal effect on particles smaller than ~50 nm as a result of interactions among aerodynamic resistance, impaction and residence time (Steffens et al., 2012). The predicted effect of wind speed by Steffens et al. (2012) agreed with the observed patterns from a later field study (Lee et al., 2018), even in terms of the critical size (predicted 50 nm versus observed 60 nm).

Most of the CFD studies do not implement separate models for pollutant removal. However, well-configured CFD models can resolve the wind flow field and allowing the estimate of air pollutant removal via atmospheric turbulence and Brownian motion near the surface. Furthermore, the effect of different species, leaf size, soil moisture content and other parameters to define canopy resistance are usually neglected in majority CFD studies. Therefore, CFD models could usually underestimate deposition and over-predict pollutant concentration.

*Hybrid models* describe combinations of two or more models which are either used in series to generate desirable outputs (Karamchandani et al., 2009; Korek et al., 2016; Sharma et al., 2013; Sun et al., 2017) or complementarily to target specific problems such as the development of modified flow fields due to complex terrain, the estimation of dry deposition because of GI, or the generation of spatial meteorological data etc. within domain (Fallahshorshani et al., 2012). Eulerian grid models, Lagrangian puff dispersion or trajectory models used along with

Gaussian plume models are classical examples of hybrid models. Globally, researchers are developing new hybrid models to simulate complex air pollutant dispersion processes under different environmental conditions. Currently, the major problem with hybrid models is the linkage between models, because of which the development of unique methodologies for linking different models and dealing with case-specific requirements linked, for example, to data availability is often required. For instance, LAI can be estimated by different models such as relating it to digital cameras values (Casadesús and Villegas, 2014), through mathematical equations linking LAI, absorbed photosynthetically active radiation and net primary production from remote sensing (Gower et al., 1999), by mathematical regression models (Blanco and Folegatti, 2003), using satellite data (Aboelghar et al., 2010; Chen et al., 2005; Xavier and Vettorazzi, 2004), and with many other direct or indirect methods (Bréda, 2003; Gower et al., 1999). Hybrid models are capable of considering GI in air pollutant concentrations simulations but because of the data required for considerations of GI (Table 2), uncertainty in data generation, spatial and temporal variation of data, there is no accepted hybrid approach for considering the GI in predicting air pollutant concentrations.

The impacts of GI on pollutant dispersion in urban areas are not considered in many microscale models. A comprehensive understanding of individual aspects, such as dry deposition (Nowak et al., 2006); filtration (Chen et al., 2017) and air pollutant concentrations redistribution (Gromke and Ruck, 2008; Miao et al., 2016) are needed to be considered in urban air quality simulation. For dry deposition, an additional sink term may be used in computational models to simulate gaseous pollutant absorption into the leaf matrix via stomata. The mathematical model used to estimate deposition, shown in Eq. (1), is applicable when the total LAD and concentration point belong to two different cells, mostly in the macroscale model. Therefore, Eqs. (2) and (3) describing a mathematical model to estimate  $V_d$  considering  $R_a$  as the resistance between the height of concentration modelled and the GI canopy are applicable for

forest canopy only. On the other hand, the microscale models, with much finer resolution and the resolving concentration around GI which has an impact of  $R_a$ , results in different  $V_d$  that at the macroscale. For instance in CFD simulation, sink term is proportional to a concentration within a cell,  $V_d$  and LAD shown in Eq. 20 (Buccolieri et al., 2018; Jeanjean et al., 2016; Vos et al., 2013) where  $V_d$  is generally assumed to be the same as macroscale.

$$S_d = -LAD \cdot V_d \cdot C \quad (20)$$

Apart from trees and hedges, surfaces like grass, soil and water also affect deposition, but this additional deposition is not considered in microscale modelling. Also, the filtration capacity of GI is the amount of gas and particles retained in its volume without absorption is neglected. This effect is most significant for particles deposition inside the GI canopy. Furthermore, the modelling of particles deposition is more complex than that of gases due to re-suspension under high wind speeds. The amount of re-suspension depends on wind speed and amount of epicuticular wax available on leaves in different seasons (Zhang et al., 2017c). Hefny et al. (2015) have discussed GI-induced aerodynamic effects with two different approaches: (i) an implicit approach (represented by surface roughness); and (ii) an explicit approach (represented by porous media) for inclusion of GI in numerical modelling, and concluded that explicit approach is more physically realistic over implicit approach for simulation of wind flow field and dispersion modelling. The built-up street canyon configuration and vortexes interaction with GI is shown in Fig 2. These vortexes in street canyons help to reduce pollutant concentrations through dilution. The flow around GI is dependent on the location of the latter in the built-up street canyon, the interaction with street canyon vortexes, the surrounding environment, and meteorological conditions. The porous behaviour of GI results in an aerodynamic effect that is different from that of solid barriers. Two zones – a low turbulence zone due to flow abatement and a high turbulence zone due to a sudden change in flow deflection – are generated due to vortexes interacting with the street GI (Vos et al., 2013).

Generally, low turbulence zones present higher concentrations, owing to relatively lesser mixing and the loss of momentum by the part of air pollutants passing through GI, getting stagnant (Santiago et al., 2017). Tong et al. (2016) employed the CFD-based CTAG model to evaluate six different vegetation barrier configurations, and identified vegetation–solid barrier combination (i.e., solid barrier followed by vegetation barrier) as one of most effective design options, *via* promoting vertical mixing (through solid barriers) and enhancing deposition (through vegetation barriers). The CTAG modeling results also revealed that a highly porous roadside vegetation barrier containing large gaps within the barrier structure could increase downwind pollutant concentrations, consistent with findings from a field study (Deshmukh et al., 2018). In conclusion, the choice of microscale model to study the impact of GI on local air pollutant concentrations simulation depends on available input parameters, simulation time, the representation of GI-pollutant interaction processes, meteorological conditions and the surrounding urban geometry.

## 5. Considerations of GI in macroscale models

Macroscale models are used to predict the air pollutant concentrations around a source, where air pollutant dispersion is dominated by meteorological and topographical conditions such as wind velocity and direction, ambient temperature, terrain slope, surface roughness and deposition. For the consideration of GI in macroscale models, important aspects are deposition velocity (Verbeke et al., 2015) and change in friction velocity and surface roughness (Barnes et al., 2014; Britter and Hanna, 2003). Here, we have reviewed methodologies for considering GI in macroscale air dispersion models. Table 4 summarises the differences in GI considerations in various macroscale models that are discussed in the subsequent text.

At macroscale, *Gaussian plume models* have been widely used for air quality prediction from a point source and have some limited applicability such as flat terrain, no local flow and

circulation and single source. Apart from inbuilt assumptions in historical Gaussian plume models such as continuous steady source, chemically inert pollutant, bell-shaped distribution of pollutants in the horizontal and vertical direction and constant meteorological conditions, for which this model category, are neither able to represent the dispersion outside these conditions nor to handle complex environmental conditions, topography, additional atmospheric chemistry and the air pollutant removal capacity of GI through dry deposition. Modified Gaussian models such as ADMS-Urban, AERMOD, CALPUFF and SCREEN3 (developed by the US-EPA) are the most commonly used amongst the scientific community. ADMS-Urban (developed by the Cambridge Environmental Research Consultants, UK) is a Gaussian plume air dispersion model that computes local flow along with turbulence due to surface roughness based on Nguyen et al. (1997) and dry deposition velocity with constant surface resistance (Apsley, 2017). With constant surface resistance, ADMS-Urban is unable to incorporate the effect of different land cover on deposition. AERMOD is a steady-state Gaussian plume model, jointly developed by the American Meteorological Society and the US-EPA, that takes meteorological inputs from AERMET (Cimorelli et al., 2005) and complex terrain data from AERMAP (Langner and Klemm, 2011). To compute deposition velocity based on Wesely (1988), AERMOD uses a constant LAI that depends on nine land use categories and five seasonal categories rather than the actual LAI that varies with the type of GI. However, Lin *et al.* (2018) have shown in their large-eddy simulation study that total particle deposition is sensitive to LAI. CALPUFF, jointly developed by Sigma Research Corporation (currently part of Earth Tech, Inc.) and California Air Research Board, is a non-steady-state Lagrangian Gaussian puff model; it uses CALMAT generated wind field or wind velocity and other inputs such as surface roughness and terrain data to compute dispersion coefficient (Bai et al., 2018). CALPUFF estimates deposition velocity without considering the  $R_{dc}$  and  $R_{ci}$  due to GI porosity and other surfaces (e.g., grass, soil) in the lower canopy that

could lead to uncertainty in dry deposition amount. These Gaussian models are therefore not capable to simulate the (i) effect of flow deflection and flow abatement near to receptor; (ii) the pollution tolerance of different GI species; (iii) characteristics (shape and dimensions) of GI types; and (iv) the effect of GI inside the urban area.

*Statistical models* are mathematical models that predict air pollutant concentrations with the help of unknown constants, which are estimated according to measured data. Such models include land use regression models (Rao et al., 2017), machine learning models (Kleine Deters et al., 2017), and Monte Carlo (Mallet and Sportisse, 2008). These models need to be trained for past datasets to assess the impact of variables in the conditions under which they were initially trained. Land use regression models have been widely used to estimate air pollutant concentrations by finding mathematical relationships between parameters such as land cover (LAI, types and spatial distribution of GI, land use pattern), meteorological data, emissions data and ambient concentrations (Cattani et al., 2017; de Hoogh et al., 2014; Habermann et al., 2015; Hoek et al., 2008; Yli-Pelkonen et al., 2017). Because these models do not consider the physical relationship between emissions and air quality under given sets of meteorological and topographical conditions (Shahraiyini and Sodoudi, 2016; Wolf et al., 2017; Zhang and Ding, 2017), the effects of GI on air pollutant concentrations remain unexplained by statistical models.

*CFD models* at macroscale require high computational time and resources, even for a smaller size of the domain but are effectively able to capture the effects of GI at a fine spatial resolution. The modelling methodology and limitations for considering GI in CFD models, box or wind tunnel models, receptor models and hybrid models were previously discussed (Section 4).

GI reduce air pollutant concentrations through pollutant removal by dry deposition and by enhancing atmospheric dilution via increased surface roughness at the urban scale. Most macroscale simulations use the average deposition value for every cell within a simulated

domain because grid size is greater than the dimension of GI that introduces uncertainty in air quality prediction. The seasonal variation leading to changes in LAI, VOC emissions, non-linear deposition behaviours and particle resuspension are important inputs, along with from meteorological data, terrain data and surface roughness, all of which need to be considered in dispersion modelling and could change air pollutant concentrations at the macroscale. Generally, deposition models estimate air pollutant removal over GI and neglect increased atmospheric dilution by their surface roughness during an assessment of GI impacts. For instance, Bodnaruk et al. (2017) used i-Tree Eco to estimate air pollutants removal over an area of 95 km<sup>2</sup> in Baltimore, US. Their modelling estimates showed an additional total pollutant (PM<sub>2.5</sub> and O<sub>3</sub>) removal of 173 t. yr<sup>-1</sup>, if the tree cover is increased from 24% in 2010 to 44.4% in 2040 (to meet the city's Baltimore sustainability plan).

## **6. Challenges in considering GI for dispersion modelling at microscale and macroscale**

Atmospheric dispersion models predict air quality under the influence of different inputs such as meteorological data, topographical data, GI data, and source emissions. Apart from the complexity of environmental processes and interface interactions (Holnicki and Nahorski, 2015; Irwin, 2014), variance in measured and estimated pollutant concentrations where GI is present may be due to: (i) pollutant measurement error; (ii) model input uncertainties (Table 2); (iii) simplification of deposition processes (Section 3); and (iv) difficulties in treating GI in numerical solutions (Sections 4 and 5). Past studies have reported the effects of input data uncertainties on pollutant concentrations at different spatial scales, including: meteorology data uncertainty at mesoscale (Gilliam et al., 2015; Godowitch et al., 2015), emissions data uncertainty at macroscale (Diez et al., 2014; Holnicki and Nahorski, 2015) and at mesoscale (Saikawa et al., 2017), topography and land use data uncertainty at macroscale (Zou et al., 2016), and surface roughness uncertainty at macroscale (Barnes et al., 2014). The challenges to model inputs and processes, especially regarding the consideration of GI in air pollutant

concentration simulations, primarily relate to: (i) spatio-temporal variation of GI characteristics such as shape and size, porosity, pollution tolerance and pollutant sink; (ii) pollutant transformation due to GI; and (iii) influences of meteorological and topographical data (such as temperature, humidity, terrain slope, wind speed and direction) on the deposition process. Uncertainties in model input data could cause predictions of air pollutant concentrations to vary up to a factor of four for identical solutions (Lohmeyer et al., 2002). The most significant challenge is the consideration of the spatio-temporal distribution of GI and its characteristics, because each GI differs from others with respect to its location, LAI, porosity, species and geometries. Past studies (Aubrun et al., 2005; Buccolieri et al., 2011; Gromke et al., 2012; Gromke and Ruck, 2008; Miao et al., 2016) have discussed the effects of GI on local wind velocity and dispersion at different spatial scale. An additional challenge is the seasonal LAI variation that affects the change in porosity and geometry of GI (wind flow alternation) and change in pollutant absorption rate (deposition velocity). GI species also exhibit different tolerances to different air pollutants (Appleton et al., 2009; Yang et al., 2015) which may cause short-term (immediately visible symptom on leaves) and long-term (premature leaf drop, reduced growth and species death) damages. Furthermore, meteorological and topographical conditions have an influence on deposition processes and are not typically included in model parameterisations. For example, the contemporary occurrence of high ozone with high temperatures (including during heat waves) and low humidity conditions, as has been reported in many studies (Filleul et al., 2006; Hou and Wu, 2016; Zhang et al., 2017b; Zhang and Wang, 2016). Similarly, elevated levels of PM<sub>2.5</sub> are reported during high temperatures and low wind speeds (Tai et al., 2010; Zhang et al., 2017b). For example, Kavassalis and Murphy (2017) have reported the coincidence of low ground-level O<sub>3</sub> concentrations and high relative humidity in the US between 1987 and 2015. This is because O<sub>3</sub> uptake is unintentionally high by plants' stomata during high relative humidity. Furthermore, Zhang et al. (2003) have

highlighted the combined effect of strong solar radiation ( $>200 \text{ W m}^{-2}$ ) and wet conditions (rainfall or morning dew) on  $R_s$  and introduce the term  $W_{st}$  (the fraction of stomatal blocking water film) in  $R_c$  calculation, Eq. (21).

$$\frac{1}{R_c} = \frac{1-W_{st}}{R_s+R_m} + \frac{1}{R_{lu}} + \frac{1}{R_{dc}+R_{cl}} + \frac{1}{R_{ac}+R_{gs}} \quad (21)$$

Pollutant transformation due to the presence of GI is another challenge in air pollution dispersion modelling. VOCs such as isoprene, monoterpenes and sesquiterpenes are released by GI and can have considerable effects on air pollutant concentrations during heat waves (Churkina et al., 2017). These VOCs can undergo chemical transformation and produce ozone and PM in the presence of high nitrogen oxide concentrations (Seinfeld and Pandis, 2006). For example, Churkina et al. (2017) reported up to ~60% and ~40% contributions in modelled ground level  $O_3$  formation from VOCs during the heat wave in July 2006 and hot summer days in 2014 in Berlin, respectively. We observed that the GI-air pollutant interaction (deposition rate) is not constant, as assumed in many dispersion models, but actually has a high spatio-temporal variation that depends on GI types and spatial distribution, as well as meteorological and climatic factors such as relative humidity, ambient temperature and wind velocity.

## 7. Linking of GI, air pollution and health outcomes

Knowledge of linkages between public health outcomes and GI-induced air pollution reduction is important to assess public health benefits (Fig. 3). We focus here on a basic framework that links GI's reduction of atmospheric pollutant concentrations and the potential exposure of individuals to assess the resultant health risk related to air pollution (Table 5). An air pollution health risk assessment (APHRA) is a mathematical approach that estimates the expected health impact of short- or long-term exposure to air pollutants in different variables such as age group, environmental conditions and socioeconomic status (WHO, 2016). Here, we present an APHRA framework to link health outcomes with short- or long- term exposure

alternation due to the presence of GI. Several epidemiological studies have reported a wide range of health impacts, such as respiratory symptoms, hospital admissions and/or premature deaths, associated with excess exposure to air pollution. These health outcomes could be quantified by a number of premature deaths, years of life lost (YLLs), disability-adjusted life years (DALYs), or change in life expectancy (Health Organization Regional Office for Europe, 2015). For instance, Pope et al. (2009) reported a life expectancy increase by 0.64 years for per  $10 \mu\text{g m}^{-3}$  decrease in  $\text{PM}_{2.5}$  for 51 US cities. The input data required to estimate the health outcomes, shown in Eq. (22), are population data ( $P$ ; numbers), baseline rates of death or hospital admission ( $M$ ; number per year), change in air pollutant concentration ( $\Delta Q$ ;  $\mu\text{g m}^{-3}$ ) and relative risk (RR) (Andre o et al., 2018; K nzli et al., 2000; Sacks et al., 2018).

$$\Delta M = (1 - e^{-RR \times \Delta Q}) \times P \times M \quad (22)$$

Where  $\Delta M$  is a change in health effects due to air pollution and RR is a change in health effect for a unit change in an air pollutant concentration. The main steps for APHRA are performed via (i) direct measurements of air pollution concentrations of individual's exposure (Steinle et al., 2015); (ii) indirect measurements by estimating pollutant concentrations with modelling or fixed site monitors (Beelen et al., 2014; Brauer et al., 2016). For APHRA, the use of the indirect method is more common over the direct method, which is mostly used in industrial or occupational health risk assessment. At a national scale study of 2425 urban and 3094 rural areas in 2010, Hirabayashi and Nowak (2016) used fixed-site monitoring data and applied pollutant concentrations change due to deposition over the tree canopy to identify air pollutant removal and health benefits with an increase in LAI or percentage of tree cover. There is uncertainty in APHRA due to factors such as: (i) the ambient air, which is a complex pollutant mixture, and making estimations of exposure assessment is challenging because monitoring stations do not map the full domain; (ii) the fact that the baseline disease burden is not properly recorded, especially for under-developed countries; and (iii) assumptions made during the

derivation of concentration-response functions such as smoking condition, indoor air pollutant exposures and medical conditions (WHO, 2016). The presence of GI could further increase uncertainty in APHRA by (i) adding allergenic pollens that may trigger other diseases, (ii) emitting bVOCs that may transform air pollutants and increase particular pollutant concentrations locally, and (iii) altering exposure by air pollutant concentration redistribution. Furthermore, USDA Forest Service developed i-Tree with BenMap (US-EPA) models provide an option to estimate the health outcomes of annual air pollutants removal by the deposition over GI canopy at the macroscale. However, changes in short-term exposure induced by pollutant concentrations redistribution at the microscale, and enhanced atmospheric pollutant dilution by increased surface roughness at the macroscale, both due to GI, have not been assessed along with deposition.

Some studies highlighted that the overall urban GI is associated with a decrease in mortality and morbidity. For instance, De Keijzer et al. (2017) linked to air pollution concentration and urban vegetation to standardized mortality rates using Poisson regression and to life expectancy using linear regression. This study was based on mortality data from 2148 small areas with an average population of 20750 inhabitants between 2009 and 2013 in Spain. An increase in life years of 0.17 (95% CI: 0.07, 0.27) with an increase in average greenness in urban areas by interquartile range was found. The same study also found a reduction in life years of 0.90 (95% CI: 0.83, 0.98), 0.20 (95% CI: 0.16, 0.24), 0.13 (95% CI: 0.09, 0.17) and 0.64 (95% CI: 0.59, 0.70) due to an increase of  $5 \mu\text{g m}^{-3}$  for each of  $\text{PM}_{10}$ ,  $\text{O}_3$ ,  $\text{NO}_x$  and  $2 \mu\text{g m}^{-3}$  in  $\text{PM}_{2.5}$ , respectively. In another study, Lovasi et al (2008) examined the association between asthma prevalence in 4 to 5 years old children and the number of street trees in New York and found that an increased tree density was associated with a 29% decrease in asthma prevalence ( $\text{RR} = 0.71$  per 343 trees  $\text{km}^{-2}$ , 95% CI: 0.64, 0.79). This association could be due to a reduction in air pollutant concentrations by urban GI. Conversely, numerous studies (King et al., 2014;

Selmi et al., 2016; Yang et al., 2008) have found air pollutant removal values between 58.9 and 99.6 kg ha<sup>-1</sup> year<sup>-1</sup> due to GI, but health benefits were not estimated, presumably owing to a lack of availability of health data.

## 8. Summary, conclusions and future outlook

We discussed various aspects related to the consideration of GI in microscale and macroscale atmospheric dispersion models. We also presented the mathematical description of different processes and the relevant inputs required to simulate GI effects for estimating air pollutant removal under deposition schemes. Microscale and macroscale air pollutant dispersion models have been surveyed with respect to their physical and chemical representations of GI into the modelling system and limitations in assessing the effects of GI on air pollutant concentrations estimation. The non-linear behaviour of GI deposition response with meteorological parameters and other challenges, such as spatio-temporal variation of GI characteristics and effects on air pollutant transformation have been briefly studied. Moreover, the importance of GI in health risk assessment through a linkage between GI, air pollution and health were examined.

Numerous numerical methods have been used to simulate additional physical and chemical processes due to the presence of GI in atmospheric dispersion models at different spatial scales, in order to estimate air pollutant removal (Section 3). These processes depend on many factors such as meteorological data, GI characteristics and air pollutant concentrations. Moreover, representing the deposition scheme in detail is complex, resource-intensive and requires a large amount of input data (such as meteorological parameters, topographical parameters, GI parameters and pollutant parameters (Table 2), which is not readily available for dispersion models. Different air pollutant dispersion methodologies used for air pollutant concentration simulations at various spatial scales have been discussed (Sections 4 and 5), and a summary of their considerations of different GI-related processes is provided in Tables 3 and 4. The

individual spatial case has specific flow, mixing characteristic and sensitivity to input parameters in simulating the effects of GI on air pollutant concentrations. It is, therefore, necessary to identify the individual spatial conditions to understand the dominating physical and chemical processes that need to be incorporated in detail during simulations of real-world problems and simplifications of various others processes to reduce computational time and resources. For instance, the predominant processes in air pollution dispersion models at microscale concern aerodynamic effects (rather than deposition), which are strongly influenced by local meteorology, source characteristics and the surrounding geometry. Therefore, the implicit approach for the inclusion of GI at microscale may lead to unrealistic predictions of air pollutant concentrations. Several other processes that also influencing deposition velocity and altering air pollutant concentrations have been reported in the literature but [many of them](#) are not represented in air pollutant concentration simulation methodologies. The vegetation emits more VOCs with rising temperatures and [can make](#) appreciable contributions to O<sub>3</sub> formation ([Section 6](#)).

The following key conclusions are drawn:

- A detailed review of parameterisation for GI modelling to estimate deposition velocity permits the conclusion that, for gaseous pollutants,  $V_d$  is dominated by  $R_c$  which is greater than  $R_a$  and  $R_b$ . Favourable conditions for gaseous pollutants to be absorbed by plant leaves depends on a series of parameters increasing LAI, size of stomata opening, photosynthesis rate per leaf area, PAR. However, for particulate matter,  $V_d$  is highly dependent on particle's diameter, as governed by a U-shaped curve which shows it's minimal for particles with sizes between 0.4 [and](#) 0.9  $\mu\text{m}$  in aerodynamic diameter.
- A synthesis of data inputs (listed in Table 2) to evaluate different resistances and deposition velocity for their estimation shows that the simplification of the deposition scheme may lead to large uncertainties in air pollutant removal estimation.

- Deposition schemes show that  $V_d$  should be treated differently for microscale and macroscale simulations because the pollutant concentrations are resolved around GI, which has the effect of  $R_a$ , in microscale models. Generally, the  $V_d$  value used in dispersion models is measured as an assumed downward flux of pollutant over GI (forest area) in the field. However, traffic emissions near roadside GI present a different configuration, where sources are located under the GI canopy.
- Usually, dispersion models (Sections 4 and 5) are not purposefully developed to assess the effects of GI on air pollutant concentrations. However, they may still be able to capture a number of processes listed in Tables 3 and 4 for GI considerations at the different spatial scales. There remains a need for coupled GI-dispersion models that can incorporate air pollutant-VOC chemistry, GI pollution tolerance and non-linear pollutant deposition under different meteorological conditions.
- The numerical framework linking GI, air pollution and health outcomes can help to estimate the benefits of GI based on a reduction in short- and long-term air pollution exposure in terms of mortality, morbidity and monetary values. These benefits are usually estimated based on the amounts of air pollutants deposited onto the surfaces of GI, and the enhanced dispersion due to surface roughness by GI (leading to dilution of pollutants) is largely overlooked.

This review identified mechanisms of air pollutant removal through the deposition process and other relevant key processes (aerodynamic effects, flow alteration and atmospheric dilution) at different spatial scales with regards to the consideration of GI in dispersion modelling. The review also highlighted a number of research questions that remain unanswered. For example, the proportional influences of deposition and dilution in reducing pollutant concentrations over large-spaced GI, such as urban parks, grassland and forests is rarely studied. Likewise, the effect of filtering capacity, pollution tolerance and temperature sensitivity of different GI types

in dispersion models require further research. The effect of wind direction on  $V_d$  in microscale simulations is not well understood. A very little is known on the modifications required in dispersion models for combined GIs such as hedges with trees and, grass with hedges or trees. We also recommend that future studies should also develop the methodologies for dispersion models that could consider the GI porosity based on the wind speed as well as considering green roofs and green walls at different spatial scales.

## 9. Acknowledgments

This work is led by the University of Surrey's GCARE team as a part of the iSCAPE (Improving Smart Control of Air Pollution in Europe) project, which is funded by the European Community's H2020 Programme (H2020-SC5-04-2015) under the Grant Agreement No. 689954. The authors from the University of Surrey, University College Dublin and the University of Bologna acknowledge the funding received from the iSCAPE project. AT and PK thanks the University of Surrey and its Department of Civil & Environment Engineering for an ORS Award and a PhD studentship to support AT's PhD research. KMZ acknowledges support from the National Science Foundation (NSF) through grant No.1605407.

## 10. References

- Abhijith, K.V., Kumar, P., 2019. Field investigations for evaluating green infrastructure effects on air quality in open-road conditions. *Atmos. Environ.* 201, 132–147.
- Abhijith, K. V., Kumar, P., Gallagher, J., McNabola, A., Baldauf, R., Pilla, F., Broderick, B., Di Sabatino, S., Pulvirenti, B., 2017. Air pollution abatement performances of green infrastructure in open road and built-up street canyon environments – A review. *Atmos. Environ.* 162, 71–86.
- Aboelghar, M., Arafat, S., Saleh, A., Naeem, S., Shirbeny, M., Belal, A., 2010. Retrieving leaf area index from SPOT4 satellite data. *Egypt. J. Remote Sens. Sp. Sci.* 13, 121–127.
- Akbari, H., Pomerantz, M., Taha, H., 2001. Cool surfaces and shade trees to reduce energy use and improve air quality in urban areas. *Sol. Energy* 70, 295–310.
- Aksu, A., 2015. Sources of metal pollution in the urban atmosphere (A case study: Tuzla, Istanbul). *J. Environ. Heal. Sci. Eng.* 13, 79.
- Alfieri, J.G., Niyogi, D., Blanken, P.D., Chen, F., LeMone, M. a., Mitchell, K.E., Ek, M.B., Kumar, A., 2008. Estimation of the Minimum Canopy Resistance for Croplands and

- Grasslands Using Data from the 2002 International H<sub>2</sub>O Project. *Mon. Weather Rev.* 136, 4452–4469.
- Amorim, J.H., Rodrigues, V., Tavares, R., Valente, J., Borrego, C., 2013. CFD modelling of the aerodynamic effect of trees on urban air pollution dispersion. *Sci. Total Environ.* 461–462, 541–551.
- Andreão, W.L., Albuquerque, T.T.A., Kumar, P., 2018. Excess deaths associated with fine particulate matter in Brazilian cities. *Atmos. Environ.* 194, 71–81.
- Appleton, B., Koci, J., Student, G., Roads, H., Harris, A.R., Sevebeck, K., Alleman, D., Swanson, L., 2009. Trees for Problem Landscape Sites -- Air Pollution [WWW Document]. URL <http://pubs.ext.vt.edu/430/430-022/430-022.html> (accessed 7.27.18).
- Apsley, D., 2017. Modelling dry deposition. Report, P17/13H/17, Cambridge Environmental Research Consultants Ltd. UK.
- Aubrun, S., Koppmann, R., Leitl, B., Möllmann-Coers, M., Schaub, A., 2005. Physical modelling of a complex forest area in a wind tunnel—comparison with field data. *Agric. For. Meteorol.* 129, 121–135.
- Awasthi, S., Khare, M., Gargava, P., 2006. General plume dispersion model (GPDM) for point source emission. *Environ. Model. Assess.* 11, 267–276.
- Bai, L., Wang, J., Ma, X., Lu, H., 2018. Air Pollution Forecasts: An Overview. *Int. J. Environ. Res. Public Health* 15, 780.
- Baik, J.-J., Park, S.-B., Kim, J.-J., 2009. Urban Flow and Dispersion Simulation Using a CFD Model Coupled to a Mesoscale Model. *J. Appl. Meteorol. Climatol.* 48, 1667–1681.
- Baldauf, R., 2017. Roadside vegetation design characteristics that can improve local, near-road air quality. *Transp. Res. Part D Transp. Environ.* 52, 354–361.
- Baldauf, R.W., Devlin, R.B., Gehr, P., Giannelli, R., Hassett-Sipple, B., Jung, H., Martini, G., McDonald, J., Sacks, J.D., Walker, K., 2016. Ultrafine Particle Metrics and Research Considerations: Review of the 2015 UFP Workshop. *J. Environ. Res. Public Heal.* 13.
- Bardelli, T., Giovannini, G., Pecchioli, L., 2011. Air quality impact of an urban park over time. *Procedia Environ. Sci.* 4, 10–16.
- Barnes, M.J., Brade, T.K., MacKenzie, A.R., Whyatt, J.D., Carruthers, D.J., Stocker, J., Cai, X., Hewitt, C.N., 2014. Spatially-varying surface roughness and ground-level air quality in an operational dispersion model. *Environ. Pollut.* 185, 44–51.
- Beelen, R., Raaschou-Nielsen, O., Stafoggia, M., Andersen, Z.J., Weinmayr, G., Hoffmann, B., Wolf, K., Samoli, E., Fischer, P., Nieuwenhuijsen, M., Vineis, P., Xun, W.W., Katsouyanni, K., Dimakopoulou, K., Oudin, A., Forsberg, B., Modig, L., Havulinna, A.S., Lanki, T., Turunen, A., Oftedal, B., Nystad, W., Nafstad, P., De Faire, U., Pedersen, N.L., Östenson, C.-G., Fratiglioni, L., Penell, J., Korek, M., Pershagen, G., Eriksen, K.T., Overvad, K., Ellermann, T., Eeftens, M., Peeters, P.H., Meliefste, K., Wang, M., Bueno-de-Mesquita, B., Sugiri, D., Krämer, U., Heinrich, J., de Hoogh, K., Key, T., Peters, A., Hampel, R., Concin, H., Nagel, G., Ineichen, A., Schaffner, E., Probst-Hensch, N., Künzli, N., Schindler, C., Schikowski, T., Adam, M., Phuleria, H., Vilier, A., Clavel-Chapelon,

- F., Declercq, C., Grioni, S., Krogh, V., Tsai, M.-Y., Ricceri, F., Sacerdote, C., Galassi, C., Migliore, E., Ranzi, A., Cesaroni, G., Badaloni, C., Forastiere, F., Tamayo, I., Amiano, P., Dorronsoro, M., Katsoulis, M., Trichopoulou, A., Brunekreef, B., Hoek, G., 2014. Effects of long-term exposure to air pollution on natural-cause mortality: an analysis of 22 European cohorts within the multicentre ESCAPE project. *Lancet* 383, 785–795.
- Belis, C.A., Karagulian, F., Larsen, B.R., Hopke, P.K., 2013. Critical review and meta-analysis of ambient particulate matter source apportionment using receptor models in Europe. *Atmos. Environ.* 69, 94–108.
- Benedict, M., McMahon, T., 2002. Green infrastructure: smart conservation for the 21st century. *Renew. Resour. J.* 20, 12–17.
- Bennett, J.H., Hill, A.C., Gates, D.M., 1973. A Model for Gaseous Pollutant Sorption by Leaves. *J. Air Pollut. Control Assoc.* 23, 957–962.
- Blanco, F.F., Folegatti, M.V., 2003. A new method for estimating the leaf area index of cucumber and tomato plants. *Hortic. Bras.* 21, 666–669.
- Bodnaruk, E.W., Kroll, C.N., Yang, Y., Hirabayashi, S., Nowak, D.J., Endreny, T.A., 2017. Where to plant urban trees? A spatially explicit methodology to explore ecosystem service tradeoffs. *Landsc. Urban Plan.* 157, 457–467.
- Bottalico, F., Chirici, G., Giannetti, F., De Marco, A., Nocentini, S., Paoletti, E., Salbitano, F., Sanesi, G., Serenelli, C., Travaglini, D., 2016. Air pollution removal by green infrastructures and urban forests in the city of Florence. *Agric. Agric. Sci. Procedia* 8, 243–251.
- Bottalico, F., Travaglini, D., Chirici, G., Garfi, V., Giannetti, F., De Marco, A., Fares, S., Marchetti, M., Nocentini, S., Paoletti, E., Salbitano, F., Sanesi, G., 2017. A spatially-explicit method to assess the dry deposition of air pollution by urban forests in the city of Florence, Italy. *Urban For. Urban Green.* 27, 221–234.
- Bowler, D.E., Buyung-Ali, L., Knight, T.M., Pullin, A.S., 2010. Urban greening to cool towns and cities: A systematic review of the empirical evidence. *Landsc. Urban Plan.*
- Brauer, M., Freedman, G., Frostad, J., van Donkelaar, A., Martin, R. V., Dentener, F., Dingenen, R. van, Estep, K., Amini, H., Apte, J.S., Balakrishnan, K., Barregard, L., Broday, D., Feigin, V., Ghosh, S., Hopke, P.K., Knibbs, L.D., Kokubo, Y., Liu, Y., Ma, S., Morawska, L., Sangrador, J.L.T., Shaddick, G., Anderson, H.R., Vos, T., Forouzanfar, M.H., Burnett, R.T., Cohen, A., 2016. Ambient Air Pollution Exposure Estimation for the Global Burden of Disease 2013. *Environ. Sci. Technol.* 50, 79–88.
- Bréda, N.J.J., 2003. Ground-based measurements of leaf area index: A review of methods, instruments and current controversies. *J. Exp. Bot.*
- Britter, R.E., Hanna, S.R., 2003. Flow and dispersion in urban areas. *Annu. Rev. Fluid Mech* 35, 469–96.
- Buccolieri, R., Salim, S.M., Leo, L.S., Di Sabatino, S., Chan, A., Ielpo, P., de Gennaro, G., Gromke, C., 2011. Analysis of local scale tree–atmosphere interaction on pollutant concentration in idealized street canyons and application to a real urban junction. *Atmos. Environ.* 45, 1702–1713.

- Buccolieri, R., Santiago, J.-L., Rivas, E., Sanchez, B., 2018. Review on urban tree modelling in CFD simulations: Aerodynamic, deposition and thermal effects. *Urban For. Urban Green.* 31, 212–220.
- Cabaraban, M.T.I., Kroll, C.N., Hirabayashi, S., Nowak, D.J., 2013. Modeling of air pollutant removal by dry deposition to urban trees using a WRF/CMAQ/i-Tree Eco coupled system. *Environ. Pollut.* 176, 123–133.
- Cape, J.N., Jones, M.R., Leith, I.D., Sheppard, L.J., van Dijk, N., Sutton, M.A., Fowler, D., 2008. Estimate of annual NH<sub>3</sub> dry deposition to a fumigated ombrotrophic bog using concentration-dependent deposition velocities. *Atmos. Environ.* 42, 6637–6646.
- Casadesús, J., Villegas, D., 2014. Conventional digital cameras as a tool for assessing leaf area index and biomass for cereal breeding. *J. Integr. Plant Biol.* 56, 7–14.
- Cattani, G., Gaeta, A., Di Menno di Bucchianico, A., De Santis, A., Gaddi, R., Cusano, M., Ancona, C., Badaloni, C., Forastiere, F., Gariazzo, C., Sozzi, R., Inglessis, M., Silibello, C., Salvatori, E., Manes, F., Cesaroni, G., 2017. Development of land-use regression models for exposure assessment to ultrafine particles in Rome, Italy. *Atmos. Environ.* 156, 52–60.
- Chen, L., Liu, C., Zhang, L., Zou, R., Zhang, Z., 2017. Variation in Tree Species Ability to Capture and Retain Airborne Fine Particulate Matter (PM<sub>2.5</sub>). *Sci. Rep.* 7, 3206.
- Chen, L., Liu, C., Zou, R., Yang, M., Zhang, Z., 2016. Experimental examination of effectiveness of vegetation as bio-filter of particulate matters in the urban environment. *Environ. Pollut.* 208, 198–208.
- Chen, X., Pei, T., Zhou, Z., Teng, M., He, L., Luo, M., Liu, X., 2015. Efficiency differences of roadside greenbelts with three configurations in removing coarse particles (PM<sub>10</sub>): A street scale investigation in Wuhan, China. *Urban For. Urban Green.* 14, 354–360.
- Chen, X., Vierling, L., Deering, D., Conley, A., 2005. Monitoring boreal forest leaf area index across a Siberian burn chronosequence: A MODIS validation study. *Int. J. Remote Sens.* 26, 5433–5451.
- Chenoweth, J., Anderson, A.R., Kumar, P., Hunt, W.F., Chimbwandira, S.J., Moore, T.L.C., 2018. The interrelationship of green infrastructure and natural capital. *Land use policy* 75, 137–144.
- Cherin, N., Roustan, Y., Musson-Genon, L., Seigneur, C., 2015. Modelling atmospheric dry deposition in urban areas using an urban canopy approach. *Geosci. Model Dev.* 8, 893–910.
- Chiesura, A., 2004. The role of urban parks for the sustainable city. *Landsc. Urban Plan.* 68, 129–138.
- Churkina, G., Kuik, F., Bonn, B., Lauer, A., Grote, R., Tomiak, K., Butler, T.M., 2017. Effect of VOC Emissions from Vegetation on Air Quality in Berlin during a Heatwave. *Environ. Sci. Technol.* 51, 6120–6130.
- Cimorelli, A.J., Perry, S.G., Venkatram, A., Weil, J.C., Paine, R.J., Wilson, R.B., Lee, R.F., Peters, W.D., Brode, R.W., 2005. AERMOD: A Dispersion Model for Industrial Source

Applications. Part I: General Model Formulation and Boundary Layer Characterization. *J. Appl. Meteorol.* 44, 682–693.

City of Sacramento, 2018. Urban Tree Canopy Assessment Sacramento, CA.

City of Woodland, 2018. Urban Tree Canopy Assessment Woodland, California 2018.

Costabile, F., Wang, F., Hong, W., Liu, F., Allegrini, I., 2006. CFD modelling of traffic-related air pollutants around an urban street-canyon in Suzhou, in: *Air Pollution XIV*, WIT Transactions on Ecology and the Environment, Vol 86. WIT Press, Southampton, UK, pp. 297–306.

Currie, B.A., Bass, B., 2008. Estimates of air pollution mitigation with green plants and green roofs using the UFORE model. *Urban Ecosyst.* 11, 409–422.

Czerniel Berndtsson, J., 2010. Green roof performance towards management of runoff water quantity and quality: A review. *Ecol. Eng.* 36, 351–360.

de Hoogh, K., Korek, M., Vienneau, D., Keuken, M., Kukkonen, J., Nieuwenhuijsen, M.J., Badaloni, C., Beelen, R., Bolignano, A., Cesaroni, G., Pradas, M.C., Cyrys, J., Douros, J., Eeftens, M., Forastiere, F., Forsberg, B., Fuks, K., Gehring, U., Gryparis, A., Gulliver, J., Hansell, A.L., Hoffmann, B., Johansson, C., Jonkers, S., Kangas, L., Katsouyanni, K., Künzli, N., Lanki, T., Memmesheimer, M., Moussiopoulos, N., Modig, L., Pershagen, G., Probst-Hensch, N., Schindler, C., Schikowski, T., Sugiri, D., Teixidó, O., Tsai, M.-Y., Yli-Tuomi, T., Brunekreef, B., Hoek, G., Bellander, T., 2014. Comparing land use regression and dispersion modelling to assess residential exposure to ambient air pollution for epidemiological studies. *Environ. Int.* 73, 382–392.

de Keijzer, C., Agis, D., Ambrós, A., Arévalo, G., Baldasano, J.M., Bande, S., Barrera-Gómez, J., Benach, J., Cirach, M., Dadvand, P., Ghigo, S., Martinez-Solanas, È., Nieuwenhuijsen, M., Cadum, E., Basagaña, X., 2017. The association of air pollution and greenness with mortality and life expectancy in Spain: A small-area study. *Environ. Int.* 99, 170–176.

Deshmukh, P., Isakov, V., Venkatram, A., Yang, B., Zhang, K.M., Logan, R., Baldauf, R., 2018. The effects of roadside vegetation characteristics on local, near-road air quality. *Air Qual. Atmos. Heal.* 1–12.

Diez, S., Barra, E., Crespo, F., Britch, J., Britch, J., 2014. Uncertainty propagation of meteorological and emission data in modeling pollutant dispersion in the atmosphere. *Ing. e Investig.* 34, 44–48.

Erismann, J.W., 1994. Evaluation of a surface resistance parametrization of sulphur dioxide. *Atmos. Environ.* 28, 2583–2594.

Erismann, J.W., Van Pul, A., Wyers, P., 1994. Parametrization of surface resistance for the quantification of atmospheric deposition of acidifying pollutants and ozone. *Atmos. Environ.* 28, 2595–2607.

Escobedo, F.J., Nowak, D.J., 2009. Spatial heterogeneity and air pollution removal by an urban forest. *Landsc. Urban Plan.* 90, 102–110.

Essa, K.S.M., 1999. Estimation of Monin-Obukhov Length Using Richardson and Bulk Richardson Number. *Conf. Nucl. Part. Phys.* 591, 591–602.

- Fallahshorshani, M., André, M., Bonhomme, C., Seigneur, C., 2012. Coupling Traffic, Pollutant Emission, Air and Water Quality Models: Technical Review and Perspectives. *Procedia - Soc. Behav. Sci.* 48, 1794–1804.
- Fernández, V., Bahamonde, H.A., Peguero-Pina, J.J., Gil-Pelegrín, E., Sancho-Knapik, D., Gil, L., Goldbach, H.E., Eichert, T., 2017. Physico-chemical properties of plant cuticles and their functional and ecological significance. *J. Exp. Bot.* 68, 5293–5306.
- Filleul, L., Cassadou, S., Médina, S., Fabres, P., Lefranc, A., Eilstein, D., Le Tertre, A., Pascal, L., Chardon, B., Blanchard, M., Declercq, C., Jusot, J.-F., Prouvost, H., Ledrans, M., 2006. The Relation Between Temperature, Ozone, and Mortality in Nine French Cities During the Heat Wave of 2003. *Environ. Health Perspect.* 114, 1344–1347.
- Fowler, D., 1981. Dry deposition of airborne pollutants on forests., in: Last, F.T., Gardiner, A.S. (Eds.), *Forest and Woodland Ecology: An Account of Research Being Done in ITE*. Cambridge, pp. 62–65.
- Gallagher, J., Baldauf, R., Fuller, C.H., Kumar, P., Gill, L.W., McNabola, A., 2015. Passive methods for improving air quality in the built environment: A review of porous and solid barriers. *Atmos. Environ.* 120, 61–70.
- Gallagher, J., Gill, L.W., McNabola, A., 2013. The passive control of air pollution exposure in Dublin, Ireland: A combined measurement and modelling case study. *Sci. Total Environ.* 458–460, 331–343.
- Ganzeveld, L., Lelieveld, J., 1995. Dry deposition parameterization in a chemistry general circulation model and its influence on the distribution of reactive trace gases. *J. Geophys. Res.* 100, 20999.
- Gardner, M.W., Dorling, S.R., 1999. Neural network modelling and prediction of hourly NO<sub>x</sub> and NO<sub>2</sub> concentrations in urban air in London. *Atmos. Environ.* 33, 709–719.
- Ghassoun, Y., Löwner, M.-O., 2017. Land use regression models for total particle number concentrations using 2D, 3D and semantic parameters. *Atmos. Environ.* 166, 362–373.
- Giardina, M., Buffa, P., 2018. A new approach for modeling dry deposition velocity of particles. *Atmos. Environ.* 180, 11–22.
- Gilliam, R.C., Hogrefe, C., Godowitch, J.M., Napelenok, S., Mathur, R., Rao, S.T., 2015. Impact of inherent meteorology uncertainty on air quality model predictions. *J. Geophys. Res. Atmos.* 120, 12,259–12,280.
- Godowitch, J.M., Gilliam, R.C., Roselle, S.J., 2015. Investigating the impact on modeled ozone concentrations using meteorological fields from WRF with an updated four-dimensional data assimilation approach. *Atmos. Pollut. Res.* 6, 305–311.
- Gong, X., Liu, H., Sun, J., Gao, Y., Zhang, X., Jha, S.K., Zhang, H., Ma, X., Wang, W., 2017. A proposed surface resistance model for the Penman-Monteith formula to estimate evapotranspiration in a solar greenhouse. *J. Arid Land* 9, 530–546.
- Goodman, J.E., Zu, K., Loftus, C.T., Lynch, H.N., Prueitt, R.L., Mohar, I., Shubin, S.P., Sax, S.N., 2018. Short-term ozone exposure and asthma severity: Weight-of-evidence analysis. *Environ. Res.* 160, 391–397.

- Gower, S.T., Kucharik, C.J., Norman, J.M., 1999. Direct and indirect estimation of leaf area index, f(APAR), and net primary production of terrestrial ecosystems. *Remote Sens. Environ.* 70, 29–51.
- Gromke, C., 2011. A vegetation modeling concept for Building and Environmental Aerodynamics wind tunnel tests and its application in pollutant dispersion studies. *Environ. Pollut.* 159, 2094–2099.
- Gromke, C., Blocken, B., 2015. Influence of avenue-trees on air quality at the urban neighborhood scale. Part II: Traffic pollutant concentrations at pedestrian level. *Environ. Pollut.* 196, 176–184.
- Gromke, C., Jamarkattel, N., Ruck, B., 2016. Influence of roadside hedgerows on air quality in urban street canyons. *Atmos. Environ.* 139, 75–86.
- Gromke, C., Ruck, B., 2008. Aerodynamic modelling of trees for small-scale wind tunnel studies. *Forestry* 81, 243–258.
- Gromke, C., Ruck, B., 2007. Influence of trees on the dispersion of pollutants in an urban street canyon—Experimental investigation of the flow and concentration field. *Atmos. Environ.* 41, 3287–3302.
- Gromke, C., Ruck, B., Gromke, C., Ruck, B., 2012. Pollutant Concentrations in Street Canyons of Different Aspect Ratio with Avenues of Trees for Various Wind Directions. *Boundary-Layer Meteorol* 144, 41–64.
- Grünhage, L., Haenel, H.-D., 1997. PLATIN (Plant-ATmosphere Interaction) I: A model of plant-atmosphere interaction for estimating absorbed doses of gaseous air pollutants. *Environ. Pollut.* 98, 37–50.
- Habermann, M., Billger, M., Haeger-Eugensson, M., 2015. Land use Regression as Method to Model Air Pollution. Previous Results for Gothenburg/Sweden. *Procedia Eng.* 115, 21–28.
- Han, Y.-J., Holsen, T.M., Hopke, P.K., Cheong, J.-P., Kim, H., Yi, S.-M., 2004. Identification of source locations for atmospheric dry deposition of heavy metals during yellow-sand events in Seoul, Korea in 1998 using hybrid receptor models. *Atmos. Environ.* 38, 5353–5361.
- Heal, M.R., Kumar, P., Harrison, R.M., 2012. Particles, air quality, policy and health. *Chem. Soc. Rev.* 41, 6606..
- Health Organization Regional Office for Europe, W., 2015. Economic cost of the health impact of air pollution in Europe Clean air, health and wealth.
- Hefny, M.S., Heinke Schlünzen, K., Grawe, D., 2015. Including trees in the numerical simulations of the wind flow in urban areas: Should we care? *J. Wind Eng. Ind. Aerodyn.* 144, 84–95.
- Hirabayashi, S., Kroll, C.N., Nowak, D.J., 2012. Development of a distributed air pollutant dry deposition modeling framework. *Environ. Pollut.* 171, 9–17.
- Hirabayashi, S., Kroll, C.N., Nowak, D.J., 2011. Urban Forest Effects-Dry Deposition ( UFORE – D ) Model Descriptions 1–23.

- Hirabayashi, S., Nowak, D.J., 2016. Comprehensive national database of tree effects on air quality and human health in the United States. *Environ. Pollut.* 215, 48–57.
- Hoek, G., Beelen, R., de Hoogh, K., Vienneau, D., Gulliver, J., Fischer, P., Briggs, D., 2008. A review of land-use regression models to assess spatial variation of outdoor air pollution. *Atmos. Environ.* 42, 7561–7578.
- Holmes, N.S., Morawska, L., 2006. A review of dispersion modelling and its application to the dispersion of particles: An overview of different dispersion models available. *Atmos. Environ.* 40, 5902–5928.
- Holnicki, P., Nahorski, Z., 2015. Emission Data Uncertainty in Urban Air Quality Modeling—Case Study. *Environ. Model. Assess.* 20, 583–597.
- Hou, P., Wu, S., 2016. Long-term Changes in Extreme Air Pollution Meteorology and the Implications for Air Quality. *Sci. Rep.* 6, 23792.
- Huang, Y., Hu, X., Zeng, N., 2009. Impact of wedge-shaped roofs on airflow and pollutant dispersion inside urban street canyons. *Build. Environ.* 44, 2335–2347.
- Irmak, S., Mutibwa, D., 2010. On the dynamics of canopy resistance: Generalized linear estimation and relationships with primary micrometeorological variables. *Water Resour. Res.* 46.
- Irwin, J.S., 2014. A suggested method for dispersion model evaluation. *J. Air Waste Manage. Assoc.* 64, 255–264.
- Jacobson, M.Z., 2005. *Fundamentals of Atmospheric Modeling*, Jurnal Ekonomi Malaysia. Cambridge University Press, Cambridge.
- Janhäll, S., 2015. Review on urban vegetation and particle air pollution – Deposition and dispersion. *Atmos. Environ.* 105, 130–137.
- Jayasooriya, V.M.M., Ng, A.W., W.M., Muthukumaran, S., Perera, B.J.C.J.C., 2017. Green infrastructure practices for improvement of urban air quality. *Urban For. Urban Green.* 21, 34–47.
- Jeanjean, A.P.R., Buccolieri, R., Eddy, J., Monks, P.S., Leigh, R.J., 2017. Air quality affected by trees in real street canyons: The case of Marylebone neighbourhood in central London. *Urban For. Urban Green.* 22, 41–53.
- Jeanjean, A.P.R., Hinchliffe, G., McMullan, W.A., Monks, P.S., Leigh, R.J., 2015. A CFD study on the effectiveness of trees to disperse road traffic emissions at a city scale. *Atmos. Environ.* 120, 1–14.
- Jeanjean, A.P.R., Monks, P.S.S., Leigh, R.J.J., 2016. Modelling the effectiveness of urban trees and grass on PM 2.5 reduction via dispersion and deposition at a city scale. *Atmos. Environ.* 147, 1–10.
- Jiang, Y., Jiang, X., Tang, R., Li, Z., Zhang, Y., Huang, C., Ru, C., 2017. Estimation of daily evapotranspiration using MODIS data to calculate instantaneous decoupling coefficient and resistances, in: 2017 IEEE International Geoscience and Remote Sensing Symposium (IGARSS). IEEE, pp. 4004–4007.

- Karamchandani, P., Lohman, K., Seigneur, C., 2009. Using a sub-grid scale modeling approach to simulate the transport and fate of toxic air pollutants, in: *Environmental Fluid Mechanics*. pp. 59–71.
- Kavassalis, S.C., Murphy, J.G., 2017. Understanding ozone-meteorology correlations: A role for dry deposition. *Geophys. Res. Lett.* 44, 2922–2931.
- Kerstiens, G., 2006. Parameterization, comparison, and validation of models quantifying relative change of cuticular permeability with physicochemical properties of diffusants. *J. Exp. Bot.* 57, 2525–2533.
- Khan, T.R., Perlinger, J.A., 2017. Evaluation of five dry particle deposition parameterizations for incorporation into atmospheric transport models. *Geosci. Model Dev* 10, 3861–3888.
- King, K.L., Johnson, S., Kheirbek, I., Lu, J.W.T., Matte, T., 2014. Differences in magnitude and spatial distribution of urban forest pollution deposition rates, air pollution emissions, and ambient neighborhood air quality in New York City. *Landsc. Urban Plan.* 128, 14–22.
- Kleine Deters, J., Zalakeviciute, R., Gonzalez, M., Rybarczyk, Y., 2017. Modeling PM<sub>2.5</sub> Urban Pollution Using Machine Learning and Selected Meteorological Parameters. *J. Electr. Comput. Eng.* 2017.
- Koloskov, G., Mukhamejanov, K., Tanton, T.W., 2007. Monin-Obukhov length as a cornerstone of the SEBAL calculations of evapotranspiration. *J. Hydrol.* 335, 170–179.
- Korek, M., Johansson, C., Svensson, N., Lind, T., Beelen, R., Hoek, G., Pershagen, G., Bellander, T., 2016. Can dispersion modeling of air pollution be improved by land-use regression? An example from Stockholm, Sweden. *J. Expo. Sci. Environ. Epidemiol.* 27, 575–581.
- Kumar, A., Chen, F., Barlage, M., Ek, M.B., Niyogi, D., 2014. Assessing Impacts of Integrating MODIS Vegetation Data in the Weather Research and Forecasting (WRF) Model Coupled to Two Different Canopy-Resistance Approaches. *J. Appl. Meteorol. Climatol.* 53, 1362–1380.
- Kumar, P., de Fatima Andrade, M., Ynoue, R.Y., Fornaro, A., de Freitas, E.D., Martins, J., Martins, L.D., Albuquerque, T., Zhang, Y., Morawska, L., 2016. New directions: From biofuels to wood stoves: The modern and ancient air quality challenges in the megacity of São Paulo. *Atmos. Environ.*
- Kumar, P., Jain, S., Gurjar, B.R., Sharma, P., Khare, M., Morawska, L., Britter, R., 2013. New Directions: Can a “blue sky” return to Indian megacities? *Atmos. Environ.*
- Kumar, P., Khare, M., Harrison, R.M., Bloss, W.J., Lewis, A.C., Coe, H., Morawska, L., 2015. New directions: Air pollution challenges for developing megacities like Delhi. *Atmos. Environ.*
- Kumar, P., Rivas, I., Sachdeva, L., 2017. Exposure of in-pram babies to airborne particles during morning drop-in and afternoon pick-up of school children. *Environ. Pollut.* 224, 407–420.
- Künzli, N., Kaiser, R., Medina, S., Studnicka, M., Chanel, O., Filliger, P., Herry, M., Horak,

- F., Puybonnieux-Textier, V., Quénel, P., Schneider, J., Seethaler, R., Vergnaud, J.-C., Sommer, H., 2000. Public-health impact of outdoor and traffic-related air pollution: a European assessment. *Lancet* 356, 795–801.
- Kwak, K.-H., Woo, S., Kim, K., Lee, S.-B., Bae, G.-N., Ma, Y.-I., Sunwoo, Y., Baik, J.-J., 2018. On-Road Air Quality Associated with Traffic Composition and Street-Canyon Ventilation: Mobile Monitoring and CFD Modeling. *Atmosphere (Basel)*. 9, 92.
- Langner, C., Klemm, O., 2011. A Comparison of Model Performance between AERMOD and AUSTAL2000. *J. Air Waste Manage. Assoc.* 61, 640–646.
- Lateb, M., Meroney, R.N., Yataghene, M., Fellouah, H., Saleh, F., Boufadel, M.C., 2016. On the use of numerical modelling for near-field pollutant dispersion in urban environments – A review. *Environ. Pollut.* 208, 271–283.
- Lee, E.S., Ranasinghe, D.R., Ahangar, F.E., Amini, S., Mara, S., Choi, W., Paulson, S., Zhu, Y., 2018. Field evaluation of vegetation and noise barriers for mitigation of near-freeway air pollution under variable wind conditions. *Atmos. Environ.* 175, 92–99.
- Lhomme, J.P., Montes, C., 2014. Generalized combination equations for canopy evaporation under dry and wet conditions. *Hydrol. Earth Syst. Sci.* 18, 1137–1149.
- Li, X.-B., Lu, Q.-C., Lu, S.-J., He, H.-D., Peng, Z.-R., Gao, Y., Wang, Z.-Y., 2016. The impacts of roadside vegetation barriers on the dispersion of gaseous traffic pollution in urban street canyons. *Urban For. Urban Green.* 17, 80–91.
- Lin, X., Chamecki, M., Katul, G., Yu, X., 2018. Effects of leaf area index and density on ultrafine particle deposition onto forest canopies: A LES study. *Atmos. Environ.* 189, 153–163.
- Litschke, T., Kuttler, W., 2008. On the reduction of urban particle concentration by vegetation – a review. *eschweizerbartxxx Meteorol. Zeitschrift* 17, 229–240.
- Liu, X., Gao, N., Hopke, P.K., Cohen, D., Bailey, G., Crisp, P., 1996. Evaluation of spatial patterns of fine particle sulfur and lead concentrations in New South Wales, Australia. *Atmos. Environ.* 30, 9–24.
- Lohmeyer, A., Mueller, W.J., Baechlin, W., 2002. A comparison of street canyon concentration predictions by different modellers: final results now available from the Podbi-exercise. *Atmos. Environ.* 36, 157–158.
- Lovasi, G.S., Quinn, J.W., Neckerman, K.M., Perzanowski, M.S., Rundle, A., 2008. Children living in areas with more street trees have lower prevalence of asthma. *J. Epidemiol. Community Heal.* 62, 647–649.
- Luber, G., McGeehin, M., 2008. Climate Change and Extreme Heat Events. *Am. J. Prev. Med.*
- Magnani, F., Leonardi, S., Tognetti, R., Grace, J., Borghetti, M., 1998. Modelling the surface conductance of a broad-leaf canopy: effects of partial decoupling from the atmosphere. *Plant, Cell Environ.* 21, 867–879.
- Maleki, H., Sorooshian, A., Goudarzi, G., Nikfal, A., Baneshi, M.M., 2016. Temporal profile of PM 10 and associated health effects in one of the most polluted cities of the world

(Ahvaz, Iran) between 2009 and 2014.

- Mallet, V., Sportisse, B., 2008. Air quality modeling: From deterministic to stochastic approaches. *Comput. Math. with Appl.* 55, 2329–2337.
- Marciotto, E.R., Oliveira, A.P., Hanna, S.R., 2010. Modeling study of the aspect ratio influence on urban canopy energy fluxes with a modified wall-canyon energy budget scheme. *Build. Environ.* 45, 2497–2505.
- Martin, N.A., Chappelka, A.H., Somers, G., Loewenstein, E.F., Keever, G.J., 2013. Evaluation of sampling protocol for i-Tree Eco: A case study in predicting ecosystem services at Auburn University. *Arboric. Urban For.* 39, 56–61.
- Massad, R.-S., Nemitz, E., Sutton, M.A., 2010. Review and parameterisation of bi-directional ammonia exchange between vegetation and the atmosphere. *Atmos. Chem. Phys.* 10, 10359–10386.
- McDonald, A.G., Bealey, W.J., Fowler, D., Dragosits, U., Skiba, U., Smith, R.I., Donovan, R.G., Brett, H.E., Hewitt, C.N., Nemitz, E., 2007. Quantifying the effect of urban tree planting on concentrations and depositions of PM<sub>10</sub> in two UK conurbations. *Atmos. Environ.* 41, 8455–8467.
- McDonald, B.C., De Gouw, J.A., Gilman, J.B., Jathar, S.H., Akherati, A., Cappa, C.D., Jimenez, J.L., Lee-Taylor, J., Hayes, P.L., McKeen, S.A., Cui, Y.Y., Kim, S.W., Gentner, D.R., Isaacman-VanWertz, G., Goldstein, A.H., Harley, R.A., Frost, G.J., Roberts, J.M., Ryerson, T.B., Trainer, M., 2018. Volatile chemical products emerging as largest petrochemical source of urban organic emissions. *Science* (80-. ). 359, 760–764.
- McPherson, E.G., Simpson, J.R., 1999. Carbon dioxide reduction through urban forestry. *Gen. Tech. Rep. PSW-171*, USDA For. Serv., Pacific Southwest Res. Station. Albany, CA.
- Meyers, T.P., Baldocchi, D.D., 1988. A comparison of models for deriving dry deposition fluxes of O<sub>3</sub> and SO<sub>2</sub> to a forest canopy. *Tellus B Chem. Phys. Meteorol.* 40, 270–284.
- Miao, H., Gopalan, H., Raghavan, V., Hee Joo, P., Joo, H., 2016. Computational Fluid Dynamics simulation of wind flow and wind force on trees in urban parks, in: 8th International Colloquium on Bluff Body Aerodynamics and Applications.
- Mohan, S.M., 2016. An overview of particulate dry deposition: measuring methods, deposition velocity and controlling factors. *Int. J. Environ. Sci. Technol.*
- Muttoo, S., Ramsay, L., Brunekreef, B., Beelen, R., Meliefste, K., Naidoo, R.N., 2018. Land use regression modelling estimating nitrogen oxides exposure in industrial south Durban, South Africa. *Sci. Total Environ.* 610–611, 1439–1447.
- Nguyen, K.C., Noonan, J.A., Galbally, I.E., Physick, W.L., 1997. Predictions of plume dispersion in complex terrain: Eulerian versus Lagrangian models. *Atmos. Environ.* 31, 947–958.
- Nowak, D.J., 1994. Air Pollution Removal by Chicago's Urban Forest, in: *Chicago's Urban Forest Ecosystem: Results of the Chicago Urban Forest Climate Project*. PA, pp. 63–81.
- Nowak, D.J., Crane, D.E., Stevens, J.C., 2006. Air pollution removal by urban trees and shrubs

in the United States. *Urban For. Urban Green.* 4, 5–123.

- Nowak, D.J., Hirabayashi, S., Bodine, A., Greenfield, E., 2014. Tree and forest effects on air quality and human health in the United States. *Env. Pollut.* 193, 119–129.
- Nowak, D.J., Hirabayashi, S., Bodine, A., Hoehn, R., 2013. Modeled PM<sub>2.5</sub> removal by trees in ten U.S. cities and associated health effects. *Environ. Pollut.* 178, 395–402.
- Nowak, D.J., Hirabayashi, S., Doyle, M., McGovern, M., Pasher, J., 2018. Air pollution removal by urban forests in Canada and its effect on air quality and human health. *Urban For. Urban Green.* 29, 40–48.
- Nowak, D.J., Hoehn, R.E., Bodine, A.R., Greenfield, E.J., O'neil-Dunne, J., Nowak, D.J., Hoehn, R.E., Greenfield, E.J., Bodine, A.R., O'neil-Dunne, J., 2013. Urban forest structure, ecosystem services and change in Syracuse, NY. *Urban Ecosyst* 19, 1455–1477.
- O'Dell, R.A., Taheri, M., Kabel, R.L., 1977. A Model for Uptake of Pollutants by Vegetation. *J. Air Pollut. Control Assoc.* 27, 1104–1109.
- Onder, S., Dursun, S., 2006. Air borne heavy metal pollution of *Cedrus libani* (A. Rich.) in the city centre of Konya (Turkey). *Atmos. Environ.* 40, 1122–1133.
- Pacitto, A., Stabile, L., Moreno, T., Kumar, P., Wierzbicka, A., Morawska, L., Buonanno, G., 2018. The influence of lifestyle on airborne particle surface area doses received by different Western populations. *Environ. Pollut.* 232, 113–122.
- Padro, J., Edwards, G.C., 1991. Sensitivity of ADOM dry deposition velocities to input parameters: A comparison with measurements for SO<sub>2</sub> and NO<sub>2</sub> over three land use types. *Atmosphere-Ocean* 29, 667–685.
- Pathak, V., Tripathi, B.D., Mishra, V.K., 2011. Evaluation of Anticipated Performance Index of some tree species for green belt development to mitigate traffic generated noise. *Urban For. Urban Green.* 10, 61–66.
- Peterson, W.B., 1980. USER'S GUIDE FOR HIWAY-2. A HIGHWAY AIR POLLUTION MODEL, U.S. Environmental Protection Agency. Washington, D.C.
- Pleijel, H., Pihl Karlsson, G., Binsell Gerdin, E., 2004. On the logarithmic relationship between NO<sub>2</sub> concentration and the distance from a highroad. *Sci. Total Environ.* 332, 261–264.
- Pope, C.A., Ezzati, M., Dockery, D.W., 2009. Fine-Particulate Air Pollution and Life Expectancy in the United States. *N. Engl. J. Med.* 360, 376–386.
- Powe, N.A., Willis, K.G., 2004. Mortality and morbidity benefits of air pollution (SO<sub>2</sub> and PM<sub>10</sub>) absorption attributable to woodland in Britain. *J. Environ. Manage.* 70, 119–128.
- Pugh, T.A.M., MacKenzie, A.R., Whyatt, J.D., Hewitt, C.N., 2012. Effectiveness of Green Infrastructure for Improvement of Air Quality in Urban Street Canyons. *Environ. Sci. Technol.* 46, 7692–7699.
- Rao, M., George, L.A., Rosenstiel, T.N., Shandas, V., Dinno, A., 2014. Assessing the relationship among urban trees, nitrogen dioxide, and respiratory health. *Environ. Pollut.* 194, 96–104.

- Rao, M., George, L.A., Shandas, V., Rosenstiel, T.N., 2017. Assessing the Potential of Land Use Modification to Mitigate Ambient NO<sub>2</sub> and Its Consequences for Respiratory Health. *Int. J. Environ. Res. Public Health* 14, 750.
- Rivas, I., Kumar, P., Hagen-Zanker, A., 2017. Exposure to air pollutants during commuting in London: Are there inequalities among different socio-economic groups? *Environ. Int.* 101, 143–157.
- Rodný, M., Nolz, R., Novák, V., Hlaváčiková, H., Loiskandl, W., Himmelbauer, M., 2016. Modified method of aerodynamic resistance calculation and its application to potential evapotranspiration estimation. *Int. Agrophysics* 30, 231–235.
- Ruggiero, A., Punzo, P., Landi, S., Costa, A., Van Oosten, M., Grillo, S., 2017. Improving Plant Water Use Efficiency through Molecular Genetics. *Horticulturae* 3, 31.
- Sacks, J.D., Lloyd, J.M., Zhu, Y., Anderton, J., Jang, C.J., Hubbell, B., Fann, N., 2018. The Environmental Benefits Mapping and Analysis Program – Community Edition (BenMAP-CE): A tool to estimate the health and economic benefits of reducing air pollution. *Environ. Model. Softw.* 104, 118–129.
- Saikawa, E., Trail, M., Zhong, M., Wu, Q., Young, C.L., Janssens-Maenhout, G., Klimont, Z., Wagner, F., Kurokawa, J., Nagpure, A.S., Gurjar, B.R., 2017. Uncertainties in emissions estimates of greenhouse gases and air pollutants in India and their impacts on regional air quality. *Environ. Res. Lett.* 12, 065002.
- Sanchez, B., Santiago, J.-L., Martilli, A., Palacios, M., Kirchner, F., 2016. CFD modeling of reactive pollutant dispersion in simplified urban configurations with different chemical mechanisms. *Atmos. Chem. Phys.* 16, 12143–12157.
- Santiago, J.-L., Rivas, E., Sanchez, B., Buccolieri, R., Martin, F., 2017. The Impact of Planting Trees on NO<sub>x</sub> Concentrations: The Case of the Plaza de la Cruz Neighborhood in Pamplona (Spain). *Atmosphere (Basel)* 8, 131.
- Schrader, F., Brümmer, C., 2014. Land Use Specific Ammonia Deposition Velocities: a Review of Recent Studies (2004–2013). *Water, Air, Soil Pollut.* 225, 2114.
- Schrader, F., Schaap, M., Zöll, U., Kranenburg, R., Brümmer, C., 2018. The hidden cost of using low-resolution concentration data in the estimation of NH<sub>3</sub> dry deposition fluxes. *Sci. Rep.* 8, 969.
- Seinfeld, J.H., Pandis, S.N., 2006. *Atmospheric Chemistry and Physics: From Air Pollution to Climate Change*, Atmospheric Chemistry and Physics.
- Selmi, W., Weber, C., Rivi re, E., Blond, N., Mehdi, L., Nowak, D., 2016. Air pollution removal by trees in public green spaces in Strasbourg city, France. *Urban For. Urban Green.* 17, 192–201.
- Shahraiyini, H.T., Sodoudi, S., 2016. Statistical Modeling Approaches for PM<sub>10</sub> Prediction in Urban Areas; A Review of 21st-Century Studies. *Atmosphere (Basel)* 7, 15.
- Shaneyfelt, K.M., Anderson, A.R., Kumar, P., Hunt, W.F., 2017. Air quality considerations for stormwater green street design. *Environ. Pollut.* 231, 768–778.

- Sharma, P., Khare, M., 2001. Modelling of vehicular exhausts - A review. *Transp. Res. Part D Transp. Environ.* 6, 179–198.
- Sharma, S., Sharma, P., Khare, M., 2013. Hybrid modelling approach for effective simulation of reactive pollutants like Ozone. *Atmos. Environ.* 80, 408–414.
- Sini, J.F., Anquetin, S., Mestayer, P.G., 1996. Pollutant dispersion and thermal effects in urban street canyons. *Atmos. Environ.* 30, 2659–2677.
- Snyder, M.G., Venkatram, A., Heist, D.K., Perry, S.G., Petersen, W.B., Isakov, V., 2013. RLINE: A line source dispersion model for near-surface releases. *Atmos. Environ.* 77, 748–756.
- Song, X.-H., Polissar, A. V., Hopke, P.K., 2001. Sources of fine particle composition in the northeastern US. *Atmos. Environ.* 35, 5277–5286.
- Steffens, J.T., Wang, Y.J., Zhang, K.M., 2012. Exploration of effects of a vegetation barrier on particle size distributions in a near-road environment. *Atmos. Environ.* 50, 120–128.
- Steinle, S., Reis, S., Sabel, C.E., Semple, S., Twigg, M.M., Braban, C.F., Leeson, S.R., Heal, M.R., Harrison, D., Lin, C., Wu, H., 2015. Personal exposure monitoring of PM 2.5 in indoor and outdoor microenvironments. *Sci. Total Environ.* 508, 383–394.
- Sun, X., Cheng, S., Li, J., Wen, W., 2017. An Integrated Air Quality Model and Optimization Model for Regional Economic and Environmental Development: A Case Study of Tangshan, China. *Aerosol Air Qual. Res.* 17, 1592–1609.
- Tai, A.P.K., Mickley, L.J., Jacob, D.J., 2010. Correlations between fine particulate matter (PM<sub>2.5</sub>) and meteorological variables in the United States: Implications for the sensitivity of PM<sub>2.5</sub> to climate change. *Atmos. Environ.* 44, 3976–3984.
- Talbi, A., Kerchich, Y., Kerbachi, R., Boughedaoui, M., 2018. Assessment of annual air pollution levels with PM<sub>1</sub>, PM<sub>2.5</sub>, PM<sub>10</sub> and associated heavy metals in Algiers, Algeria. *Environ. Pollut.* 232, 252–263.
- Tallis, M., Taylor, G., Sinnett, D., Freer-Smith, P., 2011. Estimating the removal of atmospheric particulate pollution by the urban tree canopy of London, under current and future environments. *Landsc. Urban Plan.* 103, 129–138.
- Tiwary, A., Sinnett, D., Peachey, C., Chalabi, Z., Vardoulakis, S., Fletcher, T., Leonardi, G., Grundy, C., Azapagic, A., Hutchings, T.R., 2009. An integrated tool to assess the role of new planting in PM<sub>10</sub> capture and the human health benefits: A case study in London. *Environ. Pollut.* 157, 2645–2653.
- Tong, Z., Baldauf, R.W., Isakov, V., Deshmukh, P., Max Zhang, K., 2016. Roadside vegetation barrier designs to mitigate near-road air pollution impacts. *Sci. Total Environ.* 541, 920–927.
- Venkatram, A., Snyder, M.G., Heist, D.K., Perry, S.G., Petersen, W.B., Isakov, V., 2013. Re-formulation of plume spread for near-surface dispersion. *Atmos. Environ.* 77, 846–855.
- Verbeke, T., Lathière, J., Szopa, S., de Noblet-Ducoudré, N., 2015. Impact of future land-cover changes on HNO<sub>3</sub> and O<sub>3</sub> surface dry deposition. *Atmos. Chem. Phys.* 15, 13555–13568.

- Vos, P.E.J., Maiheu, B., Vankerkom, J., Janssen, S., 2013. Improving local air quality in cities: To tree or not to tree? *Environ. Pollut.* 183, 113–122.
- Vranckx, S., Vos, P., Maiheu, B., Janssen, S., 2015. Impact of trees on pollutant dispersion in street canyons: A numerical study of the annual average effects in Antwerp, Belgium. *Sci. Total Environ.* 532, 474–483.
- Wählin, P., Berkowicz, R., Palmgren, F., 2006. Characterisation of traffic-generated particulate matter in Copenhagen. *Atmos. Environ.* 40, 2151–2159.
- Wahlina, P., Palmgren, F., Van Dingenen, R., 2001. Experimental studies of ultrafine particles in streets and the relationship to traffic. *Atmos. Environ.* 35, S63–S69.
- Walmsley, J.L., Wesely, M.L., 1996. Modification of coded parametrizations of surface resistances to gaseous dry deposition. *Atmos. Environ.* 30, 1181–1188.
- Watson, J.G., 1984. Overview of Receptor Model Principles. *J. Air Pollut. Control Assoc.* 34, 619–623.
- Watson, J.G., Zhu, T., Chow, J.C., Engelbrecht, J., Fujita, E.M., Wilson, W.E., 2002. Receptor modeling application framework for particle source apportionment, in: *Chemosphere*. Pergamon, pp. 1093–1136.
- Wesely, M., 2000. A review of the current status of knowledge on dry deposition. *Atmos. Environ.* 34, 2261–2282.
- Wesely, M.L., 1989. Parameterization of surface resistances to gaseous dry deposition in regional-scale numerical models. *Atmos. Environ.* 23, 1293–1304.
- Wesely, M.L., 1988. Improved parameterizations for surface resistance to gaseous dry deposition in regional-scale, numerical models. Report, EPA/600/3-88/025, U.S. Environmental Protection Agency.. North caroline.
- Wesely, M.L., Hicks, B.B., 1977. Some Factors that Affect the Deposition Rates of Sulfur Dioxide and Similar Gases on Vegetation. *J. Air Pollut. Control Assoc.* 27, 1110–1116.
- WHO, 2016. Health risk assessment of air pollution – general principles, *International Journal of Mass Spectrometry*. Copenhagen.
- Wolf, K., Cyrus, J., Harciníková, T., Gu, J., Kusch, T., Hampel, R., Schneider, A., Peters, A., 2017. Land use regression modeling of ultrafine particles, ozone, nitrogen oxides and markers of particulate matter pollution in Augsburg, Germany. *Sci. Total Environ.* 579, 1531–1540.
- Wong, A.Y.H., Tai, A.P.K., Ip, Y.-Y., 2018. Attribution and Statistical Parameterization of the Sensitivity of Surface Ozone to Changes in Leaf Area Index Based On a Chemical Transport Model. *J. Geophys. Res. Atmos.* 1883–1898.
- Xavier, A.C., Vettorazzi, C.A., 2004. Mapping leaf area index through spectral vegetation indices in a subtropical watershed. *Int. J. Remote Sens.* 25, 1661–1672.
- Xiao, Y., Zhu, X.-G., 2017. Components of mesophyll resistance and their environmental responses: A theoretical modelling analysis. *Plant. Cell Environ.* 40, 2729–2742.

- Yang, J., Chang, Y., Yan, P., 2015. Ranking the suitability of common urban tree species for controlling PM<sub>2.5</sub> pollution. *Atmos. Pollut. Res.* 6, 267–277.
- Yang, J., McBride, J., Zhou, J., Sun, Z., 2004. The urban forest in Beijing and its role in air pollution reduction. *Urban For. Urban Green.* 3, 65–78.
- Yang, J., Yu, Q., Gong, P., 2008. Quantifying air pollution removal by green roofs in Chicago. *Atmos. Environ.* 42, 7266–7273.
- Yin, S., Shen, Z., Zhou, P., Zou, X., Che, S., Wang, W., 2011. Quantifying air pollution attenuation within urban parks: An experimental approach in Shanghai, China. *Environ. Pollut.* 159, 2155–2163.
- Yli-Pelkonen, V., Scott, A.A., Viippola, V., Setälä, H., 2017. Trees in urban parks and forests reduce O<sub>3</sub>, but not NO<sub>2</sub> concentrations in Baltimore, MD, USA. *Atmos. Environ.* 167, 73–80.
- Zhang, J., Ding, W., 2017. Prediction of Air Pollutants Concentration Based on an Extreme Learning Machine: The Case of Hong Kong. *Int. J. Environ. Res. Public Health* 14, 114.
- Zhang, Q., Chang, M., Zhou, S., Chen, W., Wang, X., Liao, W., Dai, J., Wu, Z., 2017a. Evaluate dry deposition velocity of the nitrogen oxides using Noah-MP physics ensemble simulations for the Dinghushan Forest, Southern China. *Asia-Pacific J. Atmos. Sci.* 53, 519–536.
- Zhang, H., Wang, Y., Park, T.-W., Deng, Y., 2017b. Quantifying the relationship between extreme air pollution events and extreme weather events. *Atmos. Res.* 188, 64–79.
- Zhang, W., Wang, B., Niu, X., 2017c. Relationship between leaf surface characteristics and particle capturing capacities of different tree species in Beijing. *Forests* 8, 1–12.
- Zhang, J., Shao, Y., 2014. A new parameterization of particle dry deposition over rough surfaces. *Atmos. Chem. Phys.* 14, 12429–12440.
- Zhang, L., Brook, J.R., Vet, R., 2003. A revised parameterization for gaseous dry deposition in air-quality models. *Atmos. Chem. Phys.* 3, 2067–2082.
- Zhang, L., Brook, J.R., Vet, R., 2002. On ozone dry deposition—with emphasis on non-stomatal uptake and wet canopies. *Atmos. Environ.* 36, 4787–4799.
- Zhang, Y., Wang, Y., 2016. Climate-driven ground-level ozone extreme in the fall over the Southeast United States. *Proc. Natl. Acad. Sci.* 113, 10025–10030.
- Zhou, P., Ganzeveld, L., Rannik, Ü., Zhou, L., Gierens, R., Taipale, D., Mammarella, I., Boy, M., 2017. Simulating ozone dry deposition at a boreal forest with a multi-layer canopy deposition model. *Atmos. Chem. Phys.* 17, 1361–1379.
- Zou, B., Xu, S., Sternberg, T., Fang, X., 2016. Effect of Land Use and Cover Change on Air Quality in Urban Sprawl. *Sustainability* 8, 677.

## List of Figures

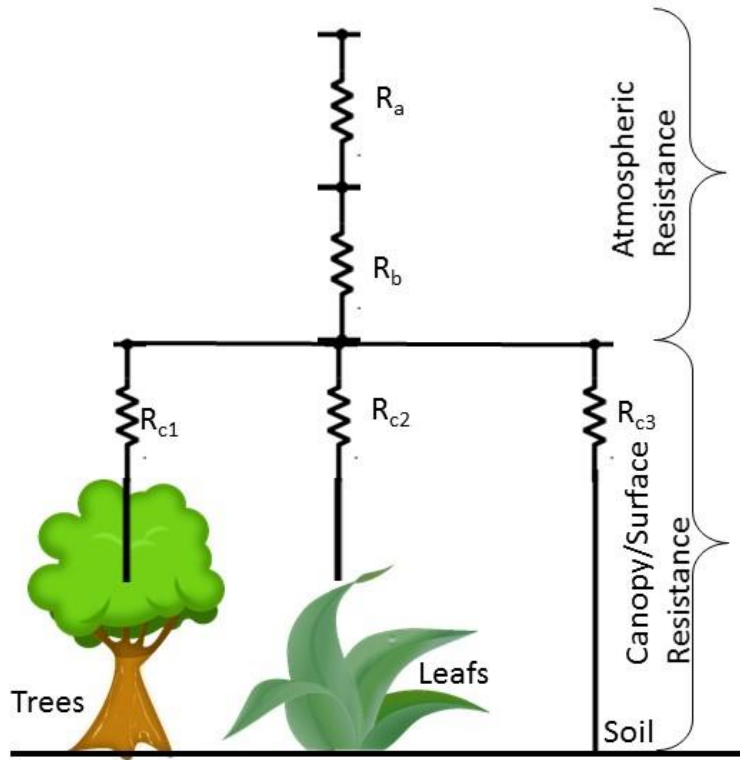


**Figure 1.** Schematic diagram showing the resistance relationship with Ohm's law in electrical circuits where  $R_a$  is aerodynamic Resistance;  $R_b$  is quasi-laminar boundary layer Resistance;  $R_c$  is canopy/surface resistance;  $R_{c1}$  is atmospheric buoyancy, lower canopy and in-canopy resistance;  $R_{c2}$  is stomatal, mesophyll and cuticular resistance; and  $R_{c3}$  is canopy soil, ground, water, snow or any other surface resistance; adopted from (Fowler, 1981).

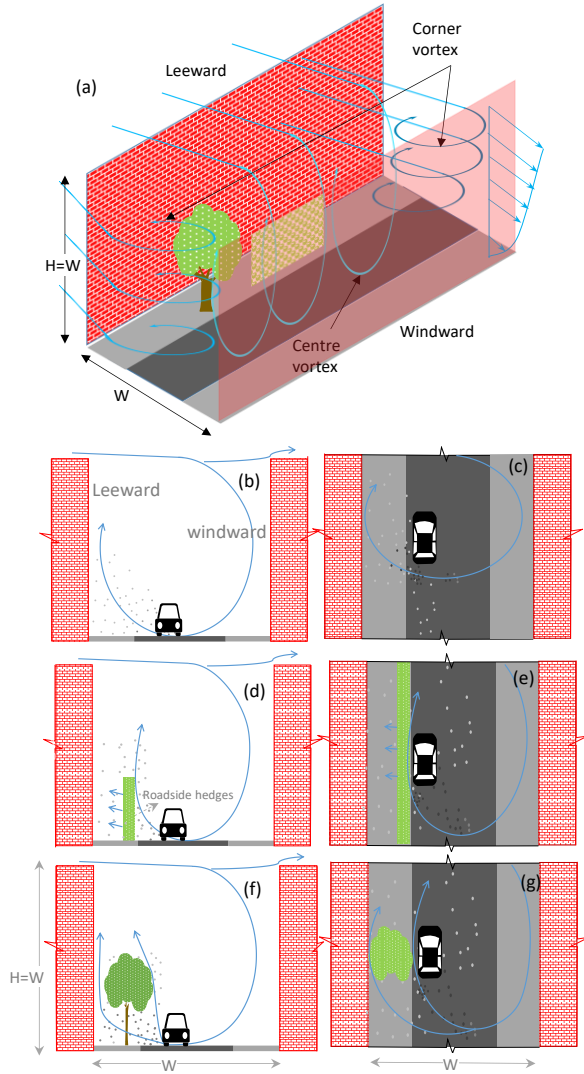


**Figure 2.** A schematic of the changes in the formation of vortex (shown by blue lines) in urban street canyon during the interaction of the flow with the leeward GI, showing vortex formation (a) in street canyon (Width/Height = 1) under perpendicular wind flow (Gromke, 2011) as well as cross-section and top view of (b, c) GI free street canyon, (c, d) street canyon with hedges, (e, f) street canyon with tree.

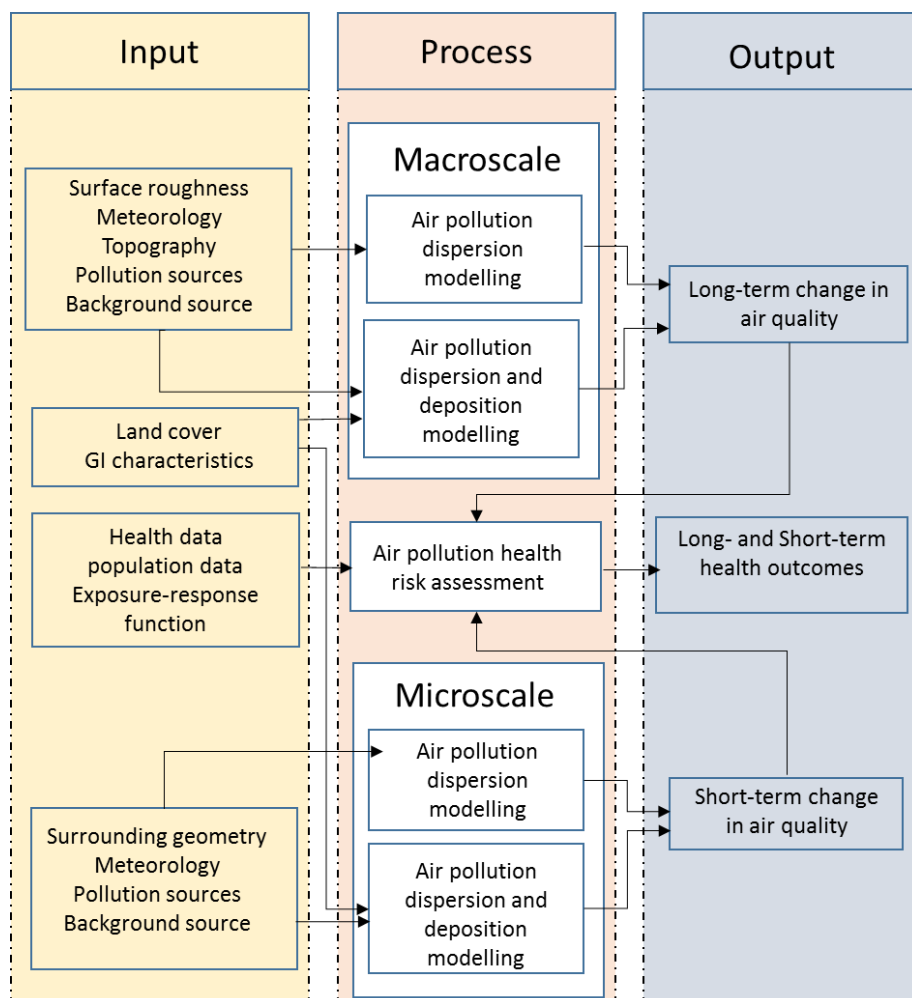


**Figure 3.** Framework for linking between GI, air pollution and public health.

## List of Tables

**Table 1.** Summary of relevant studies considering GI modelling at the microscale (street and neighbourhood) and macroscale (city).

City (modelled area)	Pollutant concentration measurement techniques	Approach for GI consideration	Author (year)
Toronto (1216 ha)	Field measurement	UFORE (i-tree)	Currie and Bass (2008)
Beijing (30,121 ha)	Field measurement	UFORE (i-tree)	Yang <i>et al.</i> (2004)
Chicago (60300 ha)	Field measurement	Nowak method (i-tree)	Nowak (1994)
Sacramento (23600 ha)	Field measurement	Mcperson method	Mcperson and Simpson (1999)
Baltimore (21000 ha)	CMAQ version 4.7.1	i-tree, CMAQ + WRF	Cabaraban <i>et al.</i> (2013)
Leicester (400 ha)	OpenFOAM software (CFD)	OpenFOAM software (CFD)	Jeanjean <i>et al.</i> (2015)
Marylebone (72 ha)	OpenFOAM software (CFD)	OpenFOAM software (CFD)	Jeanjean <i>et al.</i> (2017)
Antwerp (32 and 64 ha)	OpenFOAM software (CFD)	OpenFOAM software (CFD)	Vranckx <i>et al.</i> (2015)
Lisbon (45.50 ha)	URVE code (CFD)	URVE code (CFD)	Amorim <i>et al.</i> (2013)
Aveiro (64 ha)	URVE code (CFD)	URVE code (CFD)	Amorim <i>et al.</i> (2013)
Leicester (400 ha)	OpenFOAM software (CFD)	OpenFOAM software (CFD)	Jeanjean <i>et al.</i> (2016)
Shanghai (0.18 ha)	FLUENT (CFD)	FLUENT (CFD)	Li <i>et al.</i> (2016)
Bari (0.645 ha)	FLUENT (CFD)	FLUENT (CFD)	Buccolieri <i>et al.</i> (2011)
Santiago (96720 ha)	Field measurement	UFORE (i-tree)	Escobedo and Nowak (2009)
Shanghai (47100 ha)	Field measurement	Statistical analysis	Yin <i>et al.</i> (2011)
Florence (10200 ha)	Field measurement	iTree software	Bardelli <i>et al.</i> (2011)
Syracuse (6500 ha)	Field measurement	iTree software	Nowak <i>et al.</i> (2013)
Auburn (306 ha)	Field measurement	iTree software	Martin <i>et al.</i> (2013)
West Midland (960000 ha) and Glasgow (300000)	FRAME model	Statistical analysis	McDonald <i>et al.</i> (2007)
Berlin (200 ha)	Field measurement	Land use regression model	Ghassoun <i>et al.</i> (2017)
Strasbourg (7830 ha)	Field measurement	iTree software	Selmi <i>et al.</i> (2016)
Chicago (58830 ha)	Monitoring stations	Nowak method (iTree)	Yang <i>et al.</i> (2008)

Chapel Hill, NC (16ha)	Field measurement	CTAG (CFD)	Steffens et al.(Steffens et al., 2012)
Chapel Hill, NC and generic near-road environments (16 ha)	Field measurement	CTAG (CFD)	Tong et al.(Tong et al., 2016)
Woodside, CA	Field measurement	CTAG (CFD)	Deshmukh et al. (2018)

**Table 2.** Summary of parameters required to calculate the dry deposition over GI surfaces.

Resistance	Meteorological parameters	Topographical parameters	GI parameters	Pollutant parameters
$R_a$	Temperature; density of air; Specific heat; sensible heat; Friction velocity; Wind speed and direction	Terrain data; Building geometry	-	Source location and elevation; Source outlet velocity; Source geometry
$R_b$	Kinematic viscosity; Thermal conductivity; Air dynamic viscosity; Temperature; Cunningham factor, particle relaxation time, thermal conductivity; Heat capacity per unit volume	Land cover/use data; Surface roughness	-	Molecular diffusivity; particle diameter
$R_s$	Air temperature, solar radiation; Solar elevation angle; Diffusion and direct-beam solar radiation; Conductance-reducing effects of air temperature	The angle between the leaf and the sun	Photosynthetically Active Radiation (PAR); Leaf water potential; vapour pressure deficit, LAI; Water vapour pressure deficit;	Molecular diffusion
$R_m$	-	-	Net photosynthesis rate per leaf area; Type of species,	Henry law constant; Absolute temperature, gas constant

$R_{lu}$	Atmospheric acids; Ambient air temperature; Relative humidity; Seasonal conditions,	-	The thickness and chemical composition of leaf-surface water-layer; LAI; Pollutant concentration over leaf; Cuticle surface area; Formation, growth and fate of water films; Type of species; Age of leaf		Pollutant concentration; Rate of pollutant interaction, pollutant composition,
$R_{dc}$	Solar radiation; Solar elevation angle	Slope of the local terrain	-	-	-
$R_{cl}$	-	-	Bark area index; Porosity; Areal density; Stem area	Henry law constant; Absolute temperature; Gas constant, reactivity factor for gases; Baseline lower canopy resistance for $SO_2$ and $O_3$	
$R_{ac}$	Friction velocity; Wind speed and direction	-	Canopy height; Leaf area Index	-	
$R_{gs}$ and $R_{soil}$	Relative humidity; Ambient concentration of air pollutant and solar radiation	pH value of soil; Soil moisture content	-	-	
$R_b$ (for particles)	Schmidt number; Air kinematic viscosity; Friction velocity; Air dynamic viscosity; Stokes number; Density of air; Ambient Temperature; Relative humidity	Surface rough; Land use cover	LAI; Height of canopy	Particle's Brownian diffusivity; Cunningham factor; Particle's settling velocity; particle relaxation time; Particle diameter; Particle density;	
$V_s$	Density of air; Gravitational acceleration; Air kinematic viscosity	-	-	Particle diameter; Particle density; Cunningham factor	

**Table 3.** Summary of the consideration of differences processes in various microscale models.

Microscale models	Consideration of different process				
	Absorption	Filtration	Aerodynamic effect	GI geometry	Pollutant tolerance limit
Box and wind tunnel models	No	Yes	Yes	Yes	No
Gaussian plume models	Yes	No	No	No	No
Receptor models	Yes	Yes	No	No	No
CFD models	Yes	Yes	Yes	Yes	No
Hybrid models	Yes	No	Yes	Yes	No

**Table 4.** Summary of the consideration of different processes in various macroscale models.

Processes	Macroscale models					
	Gaussian plume models	Modified Gaussian models	Statistical models	Receptor models	CFD models	Hybrid models
Absorption	No	Yes	Yes	Yes	Yes	Yes
LAI	No	No	Yes	No	Yes	Yes
Land cover	No	Yes	Yes	No	Yes	Yes
Surface roughness	No	Yes	No	No	Yes	Yes
Terrain data	No	Yes	No	No	Yes	Yes
VOC emissions	No	No	No	No	No	No
Coupled dispersion-deposition	No	Yes	Yes	Yes	Yes	No
Background Concentration variation	No	No	No	No	No	Yes

**Table 5.** Summary of relevant studies that have quantified the linkage between GI, air pollutant

reduction and health benefits.

Author (year)	City; Model used	Summary
Tiwary et al.(2009)	London (UK); (ADMS-Urban + statistical model)	<ul style="list-style-type: none"> <li>PM<sub>10</sub> removal has been estimated through different GI combinations with two species (sycamore maple (<i>Acer pseudoplatanus</i> L.), Douglas fir (<i>Pseudotsuga menziesii</i> Franco) and grassland using computational model.</li> <li>PM<sub>10</sub> reduction varied between 0.03 to 2.33 t ha yr<sup>-1</sup> with different GI combination.</li> <li>The health effects noted were a reduction in 2 premature deaths per year and 2 respiratory hospital admissions per year.</li> </ul>
Powe and Willis (2004)	Britain(UK); (Monitoring stations+ statistical model)	<ul style="list-style-type: none"> <li>The absorption of SO<sub>2</sub> and PM<sub>10</sub> via forests (more than 2 ha in area) were estimated based on National Air Quality Information and Forest Commission spatial distribution data of woodland.</li> <li>The forest can absorb large quantity of air pollutants, for example, 385,695–596,916 metric tonnes of PM<sub>10</sub> and 7715–11,215 metric tonnes of SO<sub>2</sub> per year</li> <li>The above air pollutants reduction would be equal to 5-7 deaths per year and 4-6 hospital admission per year.</li> </ul>
David J. Nowak et al.(2013)	10 U.S. cities; (Monitoring stations + i-Tree)	<ul style="list-style-type: none"> <li>PM<sub>2.5</sub> removal was estimated for 10 U.S. cities with existing trees cover using i-Tree model and U.S. EPA monitors concentration.</li> <li>Total amount of PM<sub>2.5</sub> removal varies from 4.7 to 64.5 tonnes per year.</li> <li>The equivalent mortality reduction from 0.1 to 7.6 death per year.</li> </ul>
Nowak et al.(2018)	86 Canada cities; (Monitoring stations + i-Tree)	<ul style="list-style-type: none"> <li>The change in air pollutants (NO<sub>2</sub>, O<sub>3</sub>, PM<sub>2.5</sub>, SO<sub>2</sub>, and CO) concentration have been estimated through the iTree model and health impacts were studied.</li> <li>The total air pollutant removal was 7500 t to 21,100 t and average removal rate was 3.72 g/m<sup>2</sup>/year.</li> <li>The overall health impacts of urban trees are included avoidance of 30 human mortality in all cities.</li> </ul>
Hirabayashi and Nowak (2016)	U.S.; (Monitoring stations + i-Tree)	<ul style="list-style-type: none"> <li>Resultant changes in concentration for the four air pollutants (NO<sub>2</sub>, O<sub>3</sub>, PM<sub>2.5</sub> and SO<sub>2</sub>) were modelled by the iTree model using deciduous and evergreen trees with varying LAI and 2010 census data. US EPA's BenMAP has been used to link air quality improvement to human health improvement was estimated.</li> </ul>

		<ul style="list-style-type: none"> <li>• In urban areas, annual mean air pollutant concentration was 15.5 (<math>\mu\text{gm}^{-3}</math>) for <math>\text{NO}_2</math>, 61.7(<math>\mu\text{gm}^{-3}</math>) for <math>\text{O}_3</math>, 10.0 (<math>\mu\text{gm}^{-3}</math>) for <math>\text{PM}_{2.5}</math> and 4.9 (<math>\mu\text{gm}^{-3}</math>) for <math>\text{SO}_2</math>. Changes in concentration increased as the LAI increased but the relation is non-linear.</li> <li>• A comprehensive national database of deciduous and evergreen trees with varying LAI and its effects on air quality and human health in the United States was developed</li> </ul>
Nowak et al.(2014)	U.S.; (Monitoring stations + i-Tree)	<ul style="list-style-type: none"> <li>• Avoidable health impacts and associated economic benefits of four air pollutants (<math>\text{NO}_2</math>, <math>\text{O}_3</math>, <math>\text{PM}_{2.5}</math> and <math>\text{SO}_2</math>) removal by trees and forest in the US were estimated for 2010.</li> <li>• The estimated quantity of air pollutants removal was 17.4 million tonnes based on hourly pollution data and daily total tree cover and LAI though i-Tree model.</li> <li>• The existing trees can help in avoiding more than 850 incidences of human mortality and 670,000 incidences of acute respiratory symptoms.</li> </ul>
Rao et al.(2014)	Portland; (Monitoring stations + LUR)	<ul style="list-style-type: none"> <li>• LUR have been used to estimate a decrease in <math>\text{NO}_2</math> concentration by an urban tree in Portland.</li> <li>• The estimated removal of <math>\text{NO}_2</math> was 0.57 ppb for every 10 ha trees.</li> <li>• The annual health benefits are approximately 21,000 fewer incidences and 7000 fewer days of missed school due to asthma exacerbation for 4-12 year-olds; 54 fewer emergency visits across people of all ages; and 46 fewer cases of hospitalization due to respiratory problems triggered by <math>\text{NO}_2</math> in the elderly.</li> <li>• The potential of an urban forest to reduce the air pollutant (<math>\text{NO}_2</math>) and hence provide health benefits are approximately 7 million USD due to reduced incidence of respiratory problems.</li> </ul>
Bodnaruk et al.(2017)	Baltimore (US); (Monitoring station + i-Tree)	<ul style="list-style-type: none"> <li>• The monetary benefits of increasing tree cover from 24% to 40% have been estimated under different spatial GI distribution.</li> <li>• An additional annual 173-ton air pollutants removal was predicted at maximum potential tree cover of 44.4%.</li> <li>• The monetary benefits of these air pollutant removal on human health were estimated equal to 6.3 million USD.</li> </ul>
City of Woodland (2018)	Woodland (California); (Remote sensing + i-Tree)	<ul style="list-style-type: none"> <li>• The total air pollutants removal and monetary benefits of existing 14.5% urban tree canopy have been assessed using high-resolution aerial imagery and remote sensing software for 2010. The U.S. EPA's BenMAP Model was used to estimate monetary values resulting from changes in air pollutants concentration.</li> </ul>

		<ul style="list-style-type: none"> <li>• The analysis estimated that Woodland's tree canopy annually removing 40 tons of air pollutants (includes CO, NO<sub>2</sub>, O<sub>3</sub>, SO<sub>2</sub> and PM<sub>10</sub>) and save 15.3 million gallons of stormwater.</li> <li>• The monetary values of health benefits resulting from air pollutants removal have been estimated as equal to 1.8 million USD.</li> </ul>
City of Sacramento (2018)	Sacramento (California); (Remote sensing + i-Tree)	<ul style="list-style-type: none"> <li>• The U.S. EPA's BenMAP Model was used to estimate monetary values resulting from air pollutants removal. These removals have been estimated using high-resolution aerial imagery and remote sensing software for existing 19.1 % urban tree canopy in 2010.</li> <li>• The analysis estimated that Sacramento's tree canopy annually removing 392.4 tons of air pollutants (includes CO, NO<sub>2</sub>, O<sub>3</sub>, SO<sub>2</sub> and PM<sub>10</sub>) and save 58 million gallons of stormwater.</li> <li>• The monetary values of health benefits resulting from air pollutants removal have been estimated as equal to 18.8 million USD.</li> </ul>